IEEE Access
Multidisciplinary ⋮ Rapid Review ⋮ Open Access Journal

Received 3 March 2026, accepted 16 March 2026, date of publication 24 March 2026, date of current version 30 March 2026.

Digital Object Identifier 10.1109/ACCESS.2026.3677310

SURVEY

Simultaneous Reflection and Transmission in Metasurfaces: A Comprehensive Review

AHMED ALI UMAR[1], FARID ZUBIR[1], (Member, IEEE), MOHD FAIRUS MOHD YUSOFF[2], MUHAMMAD INAM ABBASI[3], (Senior Member, IEEE), SHAHARIL MOHD SHAH[4], (Member, IEEE), ARSHAD KARIMBU VALLAPPIL[5], MAHER ASSAAD[6], AND NOORLINDAWATY MD JIZAT[7], (Member, IEEE)

[1]Wireless Communication Centre, Faculty of Electrical Engineering, Universiti Teknologi Malaysia, Johor Bahru, Johor 81310, Malaysia
[2]Department of Communication Engineering, Faculty of Electrical Engineering, Universiti Teknologi Malaysia, Johor Bahru 81310, Malaysia
[3]Faculty of Electronics and Computer Engineering and Technology, Universiti Teknikal Malaysia Melaka, Melaka 76100, Malaysia
[4]Advanced Telecommunication Research Center, Universiti Tun Hussein Onn Malaysia, Batu Pahat, Johor 86400, Malaysia
[5]Department of Electrical Engineering, Faculty of Engineering, Islamic University of Madinah, Madinah 42351, Saudi Arabia
[6]Department of Electrical and Computer Engineering, College of Engineering and Information Technology, Ajman University, Ajman, United Arab Emirates
[7]Faculty of Artificial Intelligence and Engineering, Multimedia University, Cyberjaya, Selangor 63100, Malaysia

Corresponding authors: Farid Zubir (faridzubir@utm.my), Ahmed Ali Umar (ahmedumar@graduate.utm.my), and Noorlindawaty Md Jizat (noorlindawaty.jizat@mmu.edu.my)

This work was supported in part by the Higher Institution Centre of Excellence (HICOE), Ministry of Higher Education Malaysia through the Wireless Communication Centre (WCC), Universiti Teknologi Malaysia (UTM) under Grant R.J130000.7823.4J610; in part by the UTM Fundamental Research (UTMFR) under Grant Q.J130000.3823.23H92; in part by the EU HORIZON MSCA-SE Project TRACE-V2X under Grant 101131204; and in part by the Faculty of Artificial Intelligence and Engineering, Multimedia University (MMU), Cyberjaya, Selangor, Malaysia.

ABSTRACT The ability of metasurfaces to manipulate electromagnetic waves has drawn much attention especially with its ability to implement multifunctional structures such as simultaneous reflection and transmission. This paper discusses the fundamental principles and key design metrics such as bandwidth performance, efficiency, polarization control, frequency, and angular stability, which describe performance capabilities and limitations of metasurfaces. A wide operational bandwidth is indeed a requisite for multiple applications; while efficiency allows for energy efficient operations and optimal throughput. Additionally, polarization control and angular stability improves the performance of the metasurface, especially for dynamic environments and next generation communication systems. However, these metasurfaces have some design limitations; for example, trade-off between bandwidth and angular stability, and independent control of reflected and transmitted waves. This paper outlines these challenges and offers avenues for further innovation toward fully realizing the potential of metasurfaces in next-generation technologies.

INDEX TERMS Metasurface, reflection, transmission, angular stability, full space manipulation, polarization.

I. INTRODUCTION

Metamaterials possess unique electromagnetic (EM) properties, representing a new modality in controlling electromagnetic waves. In recent years, metamaterials have sparked considerable scientific interest due to the unique physical phenomena and novel functional devices they offer [1], [2], [3], [4], [5], [6]. However, significant manufacturing challenges and material loss impede its advancement [7]. Metasurface, [8], [9], [10], [11], [12], [13], [14] as a planar form of metamaterial, has recently evolved due to its ability to manipulate electromagnetic wavefronts in unique ways and its ease of fabrication [15]. Metasurfaces significantly reduce the fabrication needs and material loss compared to bulk metamaterials due to their small characteristic thickness, which is significantly lower than a wavelength [16]. Multipurpose electromagnetic devices are in demand as integration technology advances.

The associate editor coordinating the review of this manuscript and approving it for publication was Weiren Zhu.

Recently, many metasurfaces have demonstrated various electromagnetic capabilities, by engineering permeability and permittivity it enables the realization of devices with properties not found in nature such as absorbers [17], [18] imaging and holograms [19], [20] energy harvesting [21], [22] polarization conversion [23] and so on. Multifunctional metasurfaces are typically fabricated by strategically arranging different sizes or geometries of meta-atoms within a single layer or by stacking them across multiple layers. The need now arises for multifunctional metasurfaces to simultaneously control reflection and transmission for intricate wavefront alterations. Mostly, metasurfaces are fabricated to either reflect [24], [25] or transmit received waves [26], [27]. Inclusion of such dual functionality in a single metasurface significantly widens the scope for further development. In communication systems, this multifunctional capability improves the efficiency of signal routing and beamforming, yielding optimal data transmission. In optical systems, it creates avenues for the deployment of high profile lenses and improved holograms [28]. Because of its ability to control reflected and transmitted waves, metasurfaces can perform beam splitting, focusing, and holography in a compact and efficient manner. Additionally, it opens up myriad opportunities in wireless communication, imaging systems [29], and energy harvesting [16], [30].

Although several literature review papers summarized in Table 1 have provided different thoughts and insights on various aspect of metasurface ranging from basic tutorials to comprehensive surveys. However, this paper highlights new insights on a different topic. Many prior review literatures [31], [32], [33], and [34], primarily focus in specific domains of reconfigurable intelligent surface (RIS) applications such as machine learning based optimizations, signal processing and channel estimation. Some of these reviews such as [35] and [36] highlights the application of RIS technology for VLC and resource allocation without addressing broader design strategies, while [37], [38], [39], explores RIS performance within particular use case like hardware architecture, communication systems, and wireless sensing. Additionally, most of the reviews [31], [40], [41] focus on reflective metasurface, but a few recent studies [42], [43] have shifted their attention toward simultaneous reflection and transmission, diverging from earlier works that concentrated exclusively on reflective surfaces. However, these recent studies provide limited reportage of the core concepts, design principles and approaches, performance trade-off, applications and future directions for these metasurfaces.

This review addresses these gaps by providing a systematic overview of metasurfaces that are capable of simultaneous control of reflection and transmission. It discusses basic principles, design strategies, and practical applications of these metasurfaces. It also highlights major challenges and discusses future research directions. The review encompasses the following:

- A detailed study of the fundamentals of metasurfaces and their functionality.
- An examination of the key performance parameters and design considerations of metasurfaces.
- A comprehensive analysis of various design strategies, highlighting their advantages and limitations.
- An outline of the unresolved challenges and proposes potential research directions to unlock the full potential and benefits of multifunctional metasurfaces.

In this paper, we present a holistic overview of metasurface fundamentals, including reflective, transmissive, active, passive, and hybrid metasurfaces in section I. In section II we explain the design parameters and metrics of metasurface. Section III covers design strategies and comparison of the various design. Research Challenges, Potential solutions, and Future Directions is discussed in Section IV. Lastly with the conclusion in Section V.

II. FUNDAMENTAL PRINCIPLES OF METASURFACE

Metasurfaces are electromagnetically thin sheets engineered to manipulate electromagnetic fields distributed over a surface through a localized, subwavelength polarization responses. Such structures are to be considered as zero thickness discontinuity sheets, but not as traditional material slabs, the effect of which is described as field jumps at the sheet position. This perspective is a natural extension of the distribution based formulation of the metasurface Generalized Sheet Transition Condition (GSTC) theory in which a discontinuous field quantity f(z) of a sheet at Z=0 is expressed as a a regular plus singular (delta-function) part [45]. The generic expansion for the discontinuous sheet problem is expressed as;

$$\mathrm{F(z)} = (\mathrm{f(z)}) + \sum\nolimits_{k=0}^{N} f_k \delta^k \ (\mathrm{z}) \tag{1}$$

where the first term on the right side of equation (1) is the regular part of f, which represents the value of the function everywhere except at Z=0, and the second term is the singular part, which corresponds to the expansion over the kth derivatives of the delta distribution.

For a metasurface in the XY plane and in the Z=0 plane, discontinuities of normal and tangential components of field across the sheet describe the interaction with an incident electromagnetic excitation. In the common truncation, in which only discontinuities of first order are preserved (i.e., higher order derivative discontinuities are neglected), the metasurface boundary relations can be simplified to the GSTCs. In [45] the GSTCs are written (Eqn. (2) – (5)) in terms of the surface electric polarization density P and surface magnetic polarization density M;

$$\widehat{z} \times \Delta H = j\omega P - \widehat{z} \times \nabla M_z \tag{2}$$

$$\Delta E \times \widehat{z} = j\omega\mu_0 M - \nabla(\frac{P_z}{\varepsilon_0}) \times \widehat{z} \tag{3}$$

$$\widehat{z} \cdot \Delta D = -\nabla \cdot P \tag{4}$$

$$\widehat{z} \cdot \Delta B = -\mu_0 \nabla \cdot M \tag{5}$$

TABLE 1. Recent review papers on RIS.

Ref.	Year	Contribution
[31]	2021	Integration of Reconfigurable Intelligent Surface (RIS) into wireless network has provided cutting-edge answers to three physical layer problems; low complexity shift optimization, passive information transfer, and efficient channel state information (CSI) acquisition.
[35]	2021	Outlined possible uses and provided a study of methods for analysing performance, managing resources, and using machine learning in RIS-assisted wireless communications.
[39]	2021	RIS, reflection, hardware architecture, channel models, and practical constraints were reviewed.
[37]	2022	Provided an overview on RIS-aided sensing and localization and presented the prototype with the testing results to resolve the primary technical obstacles.
[38]	2022	From a signal processing perspective, this article provides an outline of the current state of the art in RIS outlining the basics, with emphasis on localization, and communication
[44]	2022	Presented a thorough overview of RIS-assisted wireless communications, focusing on potential solutions to actual estimation and beamforming design challenges.
[33]	2022	Reviewed IRS, addressed shortcomings in existing research, and explored IRS-related research opportunities.
[36]	2022	Presented the concept of IOS, facilitating comprehensive multidimensional communications serving users on the interface. Additionally, a novel hybrid beamforming method is introduced to enhance wireless communications utilizing using IOS framework.
[34]	2022	This IOS review addresses future cellular network applications along with beamforming, channel modelling, experimental implementation, and performance measurements
[32]	2023	Explored RIS technology for indoor VLC systems, focusing on how it solves problems with device alignment and line-of-sight (LoS) blocking.
[40]	2023	Machine learning algorithms are examined for reconfigurable intelligent surfaces, accompanied by a review of intelligent spectrum allocation in Internet of Things systems. Additionally, it examines the integration of several machine learning techniques and their potential integration into existing machine learning solutions.
[41]	2023	Presented an overview of RIS emphasizing hardware.
[42]	2023	Provided a survey on current advancement in resource allocation techniques and performance assessment methods.
[43]	2024	This review discusses the potential of reconfigurable intelligent surfaces (RIS) to support 6G networks in terahertz (THz) communication. It also reviews the efficiency of RIS, especially in reducing signal attenuation and improve diffraction performance in terahertz communications.
Our Work	2025	This review provides a systematic overview of metasurfaces designed to enable simultaneous control of reflection and transmission. The study discusses basic principles, design strategies, and identifies key challenges and future directions in the field, providing valuable insight into developing areas for further research.

Here $\Delta(\cdot)$ denotes the difference of the total fields evaluated above and just below the metasurface. These relations indicates that metasurfaces operate by the controlled electric and magnetic sheet polarizations that imprint desired discontinuities on E and H fields, rather than relying on bulk propagation phase accumulation [46].

Another approach for metasurface operations particularly for shaping wavefront is by introducing a spatial phase discontinuity at the interface as depicted in figure 1. According to the authors in [47], metasurfaces create a designed phase gradient $\partial\phi/\partial x$ which changes the balance of tangential momentum, resulting in generalized refraction/reflection laws (Eqn. (6)). Although the resultant equation is commonly expressed in the context of refraction/reflection, the general concept is that artificial gradients in tangential phase introduce an artificial transverse wavevector component to the scattered field.

$$k_{r,x} = k_{i,x} + \frac{\partial \emptyset}{\partial x},\ k_{t,x} = k_{i,x} + \frac{\partial \emptyset}{\partial x} \tag{6}$$

where $k_{i,x}$, $k_{r,x}$, and $k_{t,x}$ are the components of the incident, reflected, and transmitted wave, and $\partial\phi/\partial x$ is the phase gradient respectively. The subwavelength control of the phase response is enabled by the metasurface so that tangential wavevector of the outgoing wave is prescribed by the imposed phase gradient.

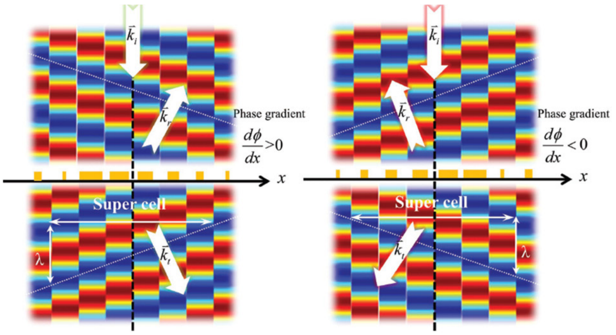

FIGURE 1. **A depiction of phase-gradient principle, where phase-gradient metasurface wavefronts are bent into arbitrary directions within their half space [47].**

In addition to propagation phase control, metasurfaces can also be based on geometric phase, where the anisotropic inclusions are mainly controlled by rotation to provide a phase response. The authors in [47] clearly calculate the rotated response by Jones-matrix operations and demonstrate how circularly polarized excitation generates a term with an extra phase of $\pm 2\theta$ which reflects the geometric phase mechanism in a form that is easy to understand.

What Are Metasurfaces

Metasurfaces are 2D engineered structures that can manipulate electromagnetic waves to create a phase shift and change the propagation of the wave [48], this is shown in figure 2. They are quite similar to their 3D counterparts i.e., metamaterials, which also derive their characteristics from volumetric structures. However, metasurfaces can generate nearly the same features while being ultra-thin [49]. One of the main guiding principles for metasurface design is the generalized Snell's law. Similar to Snell's law, taking a step further from classical reflection and refraction laws, metasurfaces can manipulate additional phase jumps across the surface [50]. This allows metasurfaces to bend, focus, and steer waves in ways that classical optics cannot achieve [51]. Once the geometry, disposition, and material properties of meta atoms are designed with an intended functionality, the technology can be customized for specific scenarios. Possible functionalities include but are not limited to: beam shaping, holography, invisibility cloaking, and polarization control [23], [52], [53]. Metasurfaces have the ability to harness and manipulate surface waves using specially engineered unit cells with distinct physical properties. They can be purposely designed to direct waves or split waves in different directions. Metasurfaces have greatly advanced the field wavefront engineering, offering lightweight planar solutions to be easily incorporated into modern electronic and photonic systems [54]. Metasurfaces function as ultra-thin lenses or beam deflectors, or even dynamically changing wavefronts, all of which cover a vast range [55], [56]. In general, all of these are of considerable interest to metasurfaces due to the unique electromagnetic properties associated with them.

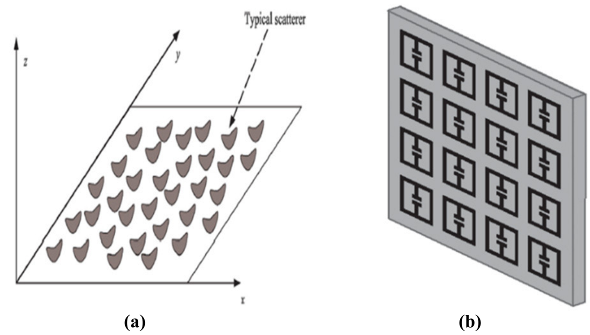

FIGURE 2. **conceptual illustrations of typical metasurface unit cell: (a) a random shaped planar array of metasurface unit cells. (b) planar arrays of metallic scatterers arranged on a substrate [57].**

A. METASURFACE FUNCTIONALITY

The behaviour of metasurfaces is governed primarily by the interactions of incoming electromagnetic waves with the surface elements. Each meta atom acts as a localized resonator that modifies the wavefront according to its shape, size, orientation, and material [58]. When these meta atoms are systematically arranged in periodic or quasi-periodic patterns, the metasurfaces can realize different optical and electromagnetic effects that include:

- Beam Steering: Steering electromagnetic waves without bulky mechanical components [59].
- Holographic Imaging: Creating three-dimensional wavefronts for display and sensing use [19].
- Polarization Control: Converting linear polarization into circular polarization and vice versa [23].
- Wave Absorption: Suppressing reflection to realize ultra-thin absorbers for stealth purposes [18].

Different designs of metasurface can lead to different effects based on the geometric arrangement of the meta-atoms and material properties. For example, a gradient metasurface changes the phase shift to steer the wave, while an anisotropic metasurface can selectively control polarization dependent behaviour [60].

B. TYPES OF METASURFACES

Metasurface can be divided into distinct types based on the functional properties they offer, table 2 summarizes the various types of metasurfaces in terms of critical design features:

1) REFLECTIVE METASURFACES

These surfaces allow control of how waves are reflected for applications such as beam reflectors, retroreflectors, and holographic surfaces [61]. When an incident wave impinges on an interface between two media, some of its energy is dissipated in the original medium. This is termed reflection. The metasurfaces use the design of meta-atoms with specific phase modifications that provide an altered angle of reflection

TABLE 2. Design features of passive, active, and hybrid metasurfaces.

Features	Passive MS Reflection/ Transmission	Active MS Reflection/ Transmission	Hybrid Reflection/ Transmission
Performance	Low	High	High
Phase Shift	Reflect/ Transmit Signal	Reflect/ Transmit Signal	Reflect/ Transmit Signal
Coverage	180^0	180^0	180^0
Design	Simple	Complex	Less complex
Energy Efficiency	High	Low	Medium

and direction of propagation of beam steering and anomalous reflection.

Reflective RIS [62] employs elements on the order of subwavelength to manipulate the phase response of the electromagnetic wave when reflected [63]. By adjusting these elements, the technology enables advanced functionalities such as beam steering [23], focusing [64], and polarization control [65], [66]. It finds its application in metasurface engineering and hence, has a potential future in next-generation communication networks due to this capability to enhance signal quality and efficiency [67]. Its lightweight, low-profile design allows deployment on different surfaces in varying environments.

2) TRANSMISSIVE METASURFACES

Transmissive metasurfaces allows a controlled passage of waves. Figure 3 shows how a wave can be propagated through metasurface into another medium. The interference pattern allows these metasurfaces to exhibit fascinating phenomena such as lensing, holography, and beam shaping by precise control of the amplitude and phase of the transmitted wave. The ability to implement transmission and reflection on the same metasurface opens up possibilities for reconfigurable and multifunctional optical devices.

Transmissive metasurface [68] provides a dynamic approach of redirecting signals as they pass through its medium, thereby optimizing the phase and amplitude of the signal efficiently [69].This configuration boost indoor coverage by redirecting outdoor signals. The transmissive metasurface manipulates and redirects signals in the surrounding environment, mitigating interferences and signal losses due to attenuation, thus providing solution for applications requiring reliable and efficient communication indoors [70].

3) PASSIVE METASURFACES

Passive metasurfaces have static properties, Passive intelligent surfaces are inexpensive and make use of electromagnetic

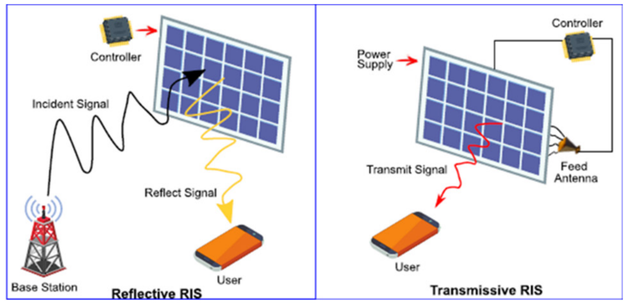

FIGURE 3. Reflective and transmissive metasurface [43].

materials that blend into their environment, enhancing wireless transmissions through passive signal reflection [62], [71], [72]. They ensure a virtual line-of-sight (LoS) and are energy efficient [73]. Nonetheless, the performance of passive metasurfaces suffers from double fading due to large path losses introduced by the multiple transmissions from the transmitter, surface, and receiver combined. This entails reduced effectiveness and comparatively less gain over systems without RIS [35].

4) ACTIVE METASURFACES

Active metasurfaces are based on a tunable mechanism such as liquid crystals or phase change materials like MEMs to adjust their wave manipulation dynamically [74]. It attempts to resolve the passive metasurface challenges by amplifying signals to counter the multiplicative fading problems [74], [75], [76]. Unlike passive metasurfaces as shown in figure 4, active RIS operates by introducing additional contrivances in the form of specialized hardware which allows active boosting of the signal strength through phase shift circuits and reflection amplifiers [77], [78]. However, this approach compromises performance with energy consumption, which can compete with conventional base station amplifiers [42]. The hybrid integration of active and passive metasurface provides a solution to manage the trade-off between optimization and energy efficiency.

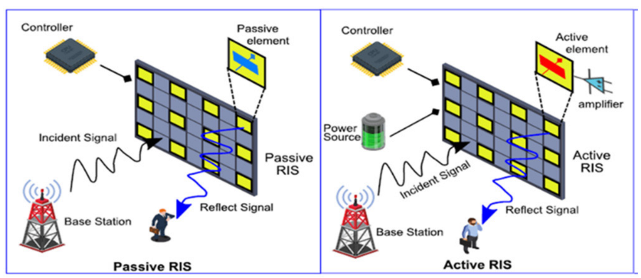

FIGURE 4. Active and passive metasurface [42].

5) HYBRID METASURFACES

Hybrid metasurface offers a compelling and flexible solution that combines the best features of active and passive technologies [79]. Active metasurface can improve real time signal processing and interference control, but the drawback of active metasurface is high power consumption particularly in off grid challenge [80]. Hybrid metasurface mitigates this by implementing active components to allow for real time dynamic adaptability, in addition to passive elements that can limit energy usage during the reflection process [81], [82]. As shown in figure 5, a smart combination of active and passive element offers a good compromise between responsiveness and efficient energy use, and it therefore fits into the rising needs of evolving wireless communication systems [83]. By virtue of its modular design, it can be adaptably deployed from next generation networks to indoor systems, thus providing a flexible approach to the implementation of performance and energy constraints [84].

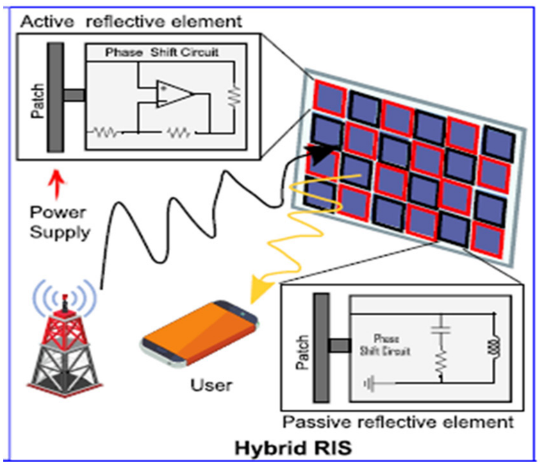

FIGURE 5. The figure illustrates the architecture of hybrid RIS [43].

C. WAVEFRONT ENGINEERING AND THE BASICS OF REFLECTION AND TRANSMISSION CONTROL

In wavefront engineering, the phase and amplitude of an electromagnetic wavefront are precisely controlled to produce the required propagation properties. This is made possible by metasurfaces, which modify the wavefront when it interacts with the surface [85]. The meta-atoms' phase shifts can be engineered to produce either constructive or destructive interference patterns, which will drive the wavefront in particular directions [86].

- **Reflection Control**

When an incident wave impinges on an interface between two media some of its energy is dissipated in the original medium, this is termed reflection. The metasurfaces use the design of meta atoms with specific phase modifications that provide an altered angle of reflection and direction of propagation of beam steering and anomalous reflection. Reflecting metasurfaces are engineered surfaces designed to manipulate the direction, polarization, and phase of reflected EM waves. They function by introducing a spatial variation of surface impedance across an interface, which leads to customized reflection behaviour. This is in accordance with the generalized Snell's law, which states that a sudden phase change at the interface can induce anomalous reflection angles [86], [87]. To engineer surface impedance, subwavelength elements such as patches, loops, or dipoles are used. The geometry of these subwavelength determines the local phase shift of the reflected wave, where each unit cell is designed to reflect the incoming wave with either delay or phase shift. Patterned arrangement of these meta-atoms, can cause the surface to bend, focus, or split the reflected wave in the desired direction [88].

As illustrated in figure 6(a), the reflectarray metasurface presented in [89] converts the spherical waves from a horn into a focused directive plane waves. It employs an element in Figure 6 (b) incorporating triple resonances that provide high efficiency and broad phase coverage. Reflecting metasurfaces have long been used in reflectarrays, which are widely applied in antenna beam steering. Initially limited by bulky 3D structures [90], the development of 2D microstrip reflectarrays [91] brought significant improvements in size, performance, and manufacturability. These metasurfaces are now crucial in applications such as such as beam steering [23], focusing [64], and polarization control [65], [66].

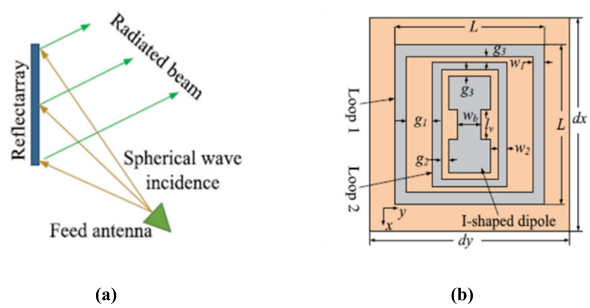

FIGURE 6. Schematics of (a) Reflectarray metasurface with spherical incident wave and (b) Top patch view of the proposed unit cell [89].

Basic Design Principles

- **Subwavelength Unit Cells**: The basic building blocks, often patch or loop structures, are smaller than the wavelength to ensure fine control [92].
- **Phase Shift**: The unit cell geometry determines the phase shift (0 to 2π), and the steepness of the phase across the surface redirects the reflected wave [93].
- **Structural Layout**: The physical layout of the metasurface is usually flat, which makes it easy to integrate into compact systems and quite portable [94].
- **Multi-Resonant Structures**: In order to increase the operational bandwidth, a multi-layered or nested elements may be employed [89].

Reflecting metasurfaces are found in antenna systems, imaging, and sensing applications. Nonetheless, they have limitations of narrow bandwidth [89], and signal losses due to material type and fabrication processes [95], [96].

- **Transmission Control**

Transmission in metasurface is simply the propagation of signals into a different medium. The unit cell pattern allows these metasurfaces to attain interesting phenomena such as lensing, holography, and beam shaping simply by manipulating the amplitude and phase of the transmitted wave. The ability to control transmission and reflection in a single structure gives the opportunities to create reconfigurable and multifunctional devices. In transmitting metasurfaces electromagnetic wave is manipulated to propagate through a medium, controlling both amplitude and phase. The design principle is based on gradient index (GRIN), where each unit cell is placed to introduces a different phase shift that can result in beam refraction, focusing, or redirection [97]. In figure 7 classical unit cell designs that use split-ring and square ring resonators (SRRs) in order to produce variable responses are depicted. These structures allows control over refractive index and polarization [98], [99], [100], as well as support electric and magnetic resonances.

A different type of transmitting metasurfaces like the Huygens' surfaces (HSFs) employs co-engineered electric and magnetic resonances to enable a highly controllable transmission of EM waves [101], [102].

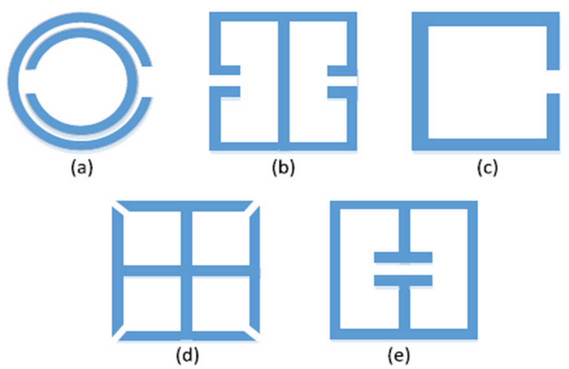

FIGURE 7. Several typical SRR elements reported in [103].

Basic Design Principles

- **Huygens' Surfaces (HSFs)**: Exploits electric and magnetic responses to shape transmitted beams [102] and minimize reflection.
- **Multi-Layer Symmetric Designs**: layered structures significantly improve transmission bandwidth and can support dual polarization [97].
- **Full Phase Control**: It is essential that each unit cell produces full phase coverage for consistent beam shaping [93], [101].
- **Polarization Conversion**: Introduction of certain structures enable polarization conversion, for example, V-antennas or anisotropic structures [104].

Transmissive metasurface [68] presents a unique and a adaptive technique of redirecting signals through its medium, effectively optimizing both the phase and amplitude [69]. This particular attribute boosts indoor coverage by harnessing nearby outdoor cellular signals. Such metasurface steers and shapes the signals into the surrounding environment, efficiently mitigating signal losses due to attenuation and interference and also presents a potential solution for high quality communication indoors [70]. Transmitting metasurfaces are effective, but are limited by some challenges such as insertion loss [105], polarization dependence [104], limited bandwidth [102], and delicate fabrication needs [106].

III. SIMULTANEOUS TRANSMITTING AND REFLECTING METASURFACES

Based on the general principles of metasurface operation and the control of reflection and transmission discussed in Section II, this section highlights some of the various structural and design strategies used to implement multifunctional metasurfaces, with emphasis on their unique implementation and performance.

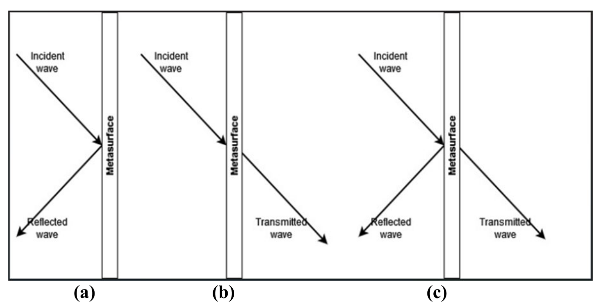

FIGURE 8. Illustration of wave interaction with metasurfaces (a) Reflecting metasurface (b) Transmitting metasurface (c) Simultaneously reflecting and transmitting metasurface.

Metasurfaces manipulate incident waves, and this happens in three distinct modes of performance: reflection, transmission, and reflection-transmission. This is illustrated in Figure 8 where (a) is operating in reflection mode, reflecting the incoming wave back to the same specified side of the interface, (b) is operating in transmission mode, it allows the incoming wave to pass through it, (c) represents metasurfaces that is designed to reflect and transmit simultaneously. In this case, the incident wave is split into a reflected and transmitted wave, and both of them can be manipulated in terms of their properties to be independent from each other. The principle of transmission and reflection design can be illustrated by generalized Snell's law [107]:

$$n_t \sin(\theta_t) - n_i \sin(\theta_i) = \frac{\lambda_0}{2\pi}\frac{d\phi}{dx} \tag{7}$$

$$n_r \sin(\theta_r) - n_i \sin(\theta_i) = \frac{\lambda_0}{2\pi}\frac{d\phi}{dx} \tag{8}$$

where θ_t *and* θ_r are the refraction and reflection angle, n_t and n_r are the refractive indexes of the incident and output medium, θ_i is the angle of incidence, and $\frac{d\phi}{dx}$ indicates the phase gradient along the interface. When the angle of incidence is 0^0, that is in free space, $n_t = n_r = n_i = 1$, the formular can be written as:

$$\theta_t = \sin^{-1}(\frac{\lambda_0}{pN}) \tag{9}$$

$$\theta_r = \sin^{-1}(\frac{\lambda_0}{pN}) \tag{10}$$

where p represents the length of the unit cell, and N the number of unit cells.

Simultaneous control of reflected and transmitted electromagnetic waves extends the functionality of metasurfaces beyond traditional single mode operation to allow full space wave manipulation of the waves in a planar structure. In practice, this ability is especially useful in situations where electromagnetic energy should be redistributed instead of merely redirected it. In wireless communication systems, simultaneous use of reflection and transmission enables the enhancement of coverage to users on both sides of a surface to enable better spatial use without the use of multiple distinct devices. In sensing and imaging applications, independent control of the wave enables multifunctional operation such as polarization conversion in transmission while maintaining reflective beam shaping. Furthermore, in compact and integrated systems, it enhances design flexibility and reduces structural redundancy. These practical implications demonstrate why it is necessary to design metasurfaces that would have the ability to control reflection and transmission. One crucial factor to be considered, is to realize such design without compromising performance, and effective design needs.

A. DESIGN STRATEGIES FOR SIMULTANEOUS REFLECTION AND TRANSMISSION

A more flexible and efficient wave manipulation is achieved due to metasurfaces ability to reflect and transmit signals simultaneously. However, a careful engineering and different design approaches is required to realize this dual functionality in a practical and scalable way.

Reflecting and transmitting metasurfaces, offer unique benefits, integrating the strengths of both, researchers are already working on multifunctional metasurfaces that can simultaneously and reasonably perform both functions on a single structure. The goal in designing such metasurface is to achieve control of phase, amplitude, and polarization in both channels while maintaining efficiency. Here are some design approaches:

1) HUYGENS' METASURFACES

Unlike designs that depend on phase compensation across varying polarization states, Huygens' metasurface prioritize impedance matching at the interface while ensuring polarization insensitivity [101]. This undoubtedly enables co-excitation of electric and magnetic dipole moments [108]. As stated by the surface equivalence principle, the electric and magnetic surface currents are essential to achieve the intended field distribution and boundary conditions, this is shown in figure 9 (a), and (c). Hence, it is necessary to handle the field discontinuities by applying the following relation for best results [109]:

$$\vec{J}_s = \widehat{n} \times (\vec{H}_2 - \vec{H}_1) \tag{11}$$

$$\vec{M}_s = -\widehat{n} \times (\vec{E}_2 - \vec{E}_1) \tag{12}$$

Here, $\vec{J}_s$ and $\vec{M}_s$ represents the surface electric and magnetic currents, respectively. Usually, a patterned metallic structure is placed on a substrate to achieve the desired impedance for the unit. A universal technique has been proposed that could alter the phase distributions of transmission and reflection required for effective surface profiles for Huygens' metasurfaces. This technique could revolutionize the capability and performance of these materials. A high contrast transmit/reflect arrays was developed using a robust high-index layer to improve performance and reduce transmission loss [110].

Early Huygen's metasurfaces were designed with pure wire and loop unit cells, as depicted in figure 9 (b), but the evolution of this field allows for in-depth research [111]. Currently, researchers are implementing all types designs with meta-atoms, omega-shaped, spiral shapes, and cascaded layered configurations yielding interesting possibilities. layered metallic structures have unique capacitive and inductive properties it allows effective manipulation of the impedance and admittance. The authors of [111] applied a dual layer metasurface to decrease the total thickness, with the unit cells designed for independent control over amplitude and phase of EM waves. The design uses orthogonal polarization to provide dual band functionality with minimum coupling. Results show very high transmission and reflection efficiency across both frequencies but limited bandwidth in the design due to a few specific operational frequency ranges. The metasurface exhibited excellent performance across the two frequency bands. However, there are restrictions due to the nature of metamaterial resonance in establishing a bandwidth. The design in [109] establishes a connection between electric (Je) and magnetic (Jm) resonances, enhancing the metasurfaces performance concerning manipulating phase, amplitude, and polarization of waves. By appropriately tuning coupling strength and phase difference between these resonances, the transformability of polarized waves and the manipulation of wavefront can be achieved. The metasurface had been designed to split an incoming polarized wave into transmitted and reflected waves cross polarized to the incidence wave. Unless properly designed, only two layers of metal resonated only with low coupling, but placement of approximately distance away on different planes expected high coupling to enhance transmission and reflection efficiency. The design permits controlling reflection and transmission independently at the same frequency.

A three-layer configuration was presented in [114], it features two identical gold rectangles on either side of a dielectric layer, with a gold resonator strategically positioned in the centre. The intermediate dielectric layer offers an exceptional capability for tuning the metasurface's admittance without altering its impedance, giving it an edge

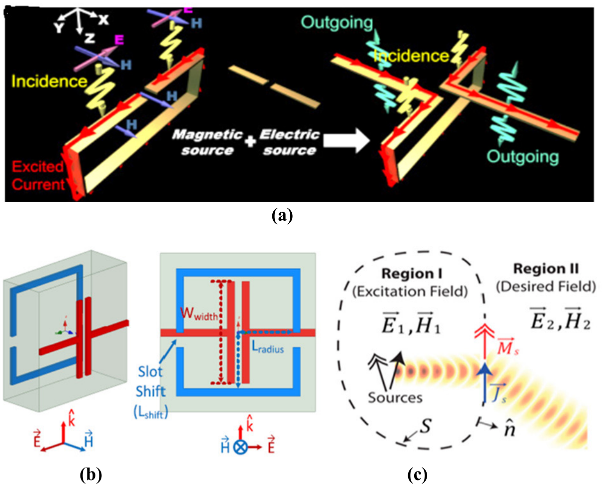

FIGURE 9. (a) Schematic of the element of the polarization conversion device based on Huygen's principle [109] (b) Omega-Bianisotropic wire-loop Huygens unit cell [112] (c) The surface equivalence principle for boundary conditions [113].

in performance. By carefully selecting the surface impedance and admittance, the structure can use the metasurface resonators in an effective way, thus reaching certain heights of excellence. Gold was chosen as the resonator material driven by the BCB dielectric layer for optimum results with no lower losses, as well as the enriching structure. Variable lengths of resonators switch the metasurface between transmission (refraction) and reflection modes with equal efficiency. This deliberate design promises minimally dissipative wave manipulation with efficiencies over 60% in both reflection and transmission modes. Metasurface design is fine-tuned for 0.83 THz and a stated bandwidth. Though it is also worth mentioning that performance is affected at oblique incident angles essentially by changes in impedance matching. Four-unit cells were also designed in [115] to produce uniform quantization of phase in 2 bits in the transmission and reflection process; to fabricate this structure, a three-layer model consisting of two dielectric slabs and three impedance sheets was utilized. Applying the boundary conditions and equivalence principle guaranteed the same transmission and reflection coefficients, thus establishing relationships between electric admittance and magnetic impedance. The proposed unit cells demonstrate effective operation over a 13% relative bandwidth with minimal variation in transmission and reflection coefficients. This setup allows a normally incident plane wave to be evenly divided into transmitted and reflected components, while enabling arbitrary phase shifts in the scattered waves. Phase coupling between transmission and reflection indicates that in the optimization of one, there is a direct effect on the other, this could limit design options for some applications.

2) PANCHARATNAM-BERRY

Pancharatnam-Berry (PB) phase signifies a notable development in geometric phases regardless of material resonance or wavelength, resulting from the spatial variation of wave polarization or orientation. Pancharatnam-Berry (PB) phase was first presented by S. Pancharatnam in 1956 and then enhanced by Sir Michael Berry in 1984 accurately manipulates wavefronts. The allows tuning of the wave's phase and amplitude in simultaneous reflection and transmission designs with high accuracy. The unique arrangement of the meta-atoms produces a distinct phase change with respect to its rotation angle, resulting in dynamic wavefront modification as long as the metasurface elements are arranged in a specific configuration. This process improves the capabilities of dual-wave regulation and optimization in designs. A ground-breaking, ultrathin single layer metasurface operating efficiently along an ultra-wideband spectrum within the modes of transmission and reflection has been revealed in [116]. The metasurface achieves impressive manipulation of the waves by harnessing the Pancharatnam Berry phase control and adopts unique scatter designs that minimize its thickness. Made of Z-shaped metallic scatterers covered with a ring-shaped copper shell, it allows several resonant electric dipole modes activated by its asymmetric geometry, leading to extraordinary operation over ultra-wide bandwidth. This photo illuminating metasurface can achieve simultaneous control of transmission and reflection and operates over a wide frequency band across 9.3 to 32.5 GHz, yielding a remarkable bandwidth of 112%. It works nicely to control circularly polarized incident waves, but functionality is reduced for arbitrary polarization states due to its specialization.

Through an alternating use of propagation phases and Pancharatnam Berry (PB) phase modification, authors in [117] proposed a metasurface that utilizes both propagation phases and Pancharatnam Berry (PB) phase modification to achieve two distinct functionalities. A frequency-selective surface (FSS) operates effectively at two specific frequency ranges approximately 18 GHz for reflection and 12 GHz for transmission facilitating the I-shaped patch employed in the design for PB phase control. As shown in figure 10, to control the PB phase, the FS-MS is composed of multilayer structures with I-shaped patches that can change orientation. The performance of the PB phase is enhanced by the inclusion of propagation phases through the frequency selective surface (FSS) in the design. The system performs well in specific frequency bands, but it may not function effectively over larger bandwidths if further design considerations are not made. To reflect and propagate waves across a range of frequency bands, the authors in [118] present a metasurface that makes use of a meta-film with ring slots. This metasurface is partitioned into regions for reflection and transmission, each featuring unique designs to fulfil particular roles. It comprises two categories of meta-atoms: R0 for reflective units and R1 for transmissive units. To reduce radar cross-section (RCS) at lower frequencies, especially in the 5.9 to 10.1 GHz range, the reflection units are fabricated as artificial magnetic conductors (AMC). For higher frequencies, 15.5 to 15.7 GHz, the transmission units use PB phase techniques to manipulate circularly polarized (CP) waves, facilitating beam deflection.

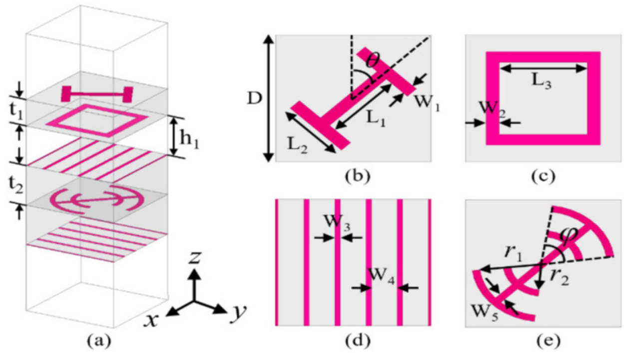

FIGURE 10. **(a) 3D view of the proposed design. (b) Top patch view (c) Bottom patch view (d) Polarizer unit, and (e) polarization converter [117].**

A 3D reflection/transmission integrated (TRI) designed to control left hand circularly polarized (LHCP) and right hand circularly polarized (RHCP) mode, shown in figure 11 was reported in [119]. The design consists of meta atoms made of linearly polarized patches with phase delay lines connecting the patches. Adaptive phase control for both LHCP and RHCP channels is accomplished by altering the dimensions of these patches and rotating the meta-atoms. The global rotation of meta-atoms facilitates Pancharatnam Berry (PB) phase shifting, thereby decoupling the left handed circularly polarized (LHCP) and right handed circularly polarized (RHCP) channels in the reflection domain. In the transmission domain, local rotation of the transmitting element induces contrasting geometric phase shifts for LHCP and RHCP components, hence enabling their differentiation. This technique facilitates independent phase manipulation of LHCP and RHCP channels, hence augmenting adaptability in both operational modes.

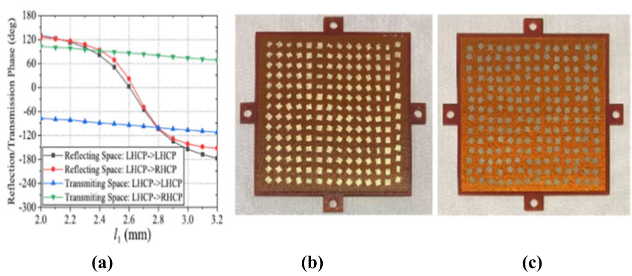

FIGURE 11. **(a) Phase response of LHCP and RHCP components under LHCP incident wave varying l_1 values. (b) Front layer (c) Back layer [119].**

3) FABRY-PEROT CAVITIES

Optical resonators known as Fabry-Perot cavities are a sandwich of a metasurface between two reflecting surfaces. This configuration produces high-quality resonances that intensifies the interaction between light and the metasurface [120]. It is a legitimate technique for wavefront manipulation because it provides exact control of the phase and amplitude of transmitted and reflected waves. In order to achieve nearly 100% efficiency, a new ultrathin metasurface has been presented in [121] that allows dynamic manipulation of reflected and transmitted phases and amplitudes. In the design exhibited in figure 12 the unit cell incorporates a double-split-ring resonator (DSRR) at its core. This device uses two orthogonally polarized metallic gratings to construct a Fabry Perot cavity. The authors are able to independently regulate the phase and amplitude of the wave by altering geometrical characteristics of the DSRR, such as its size and orientation.

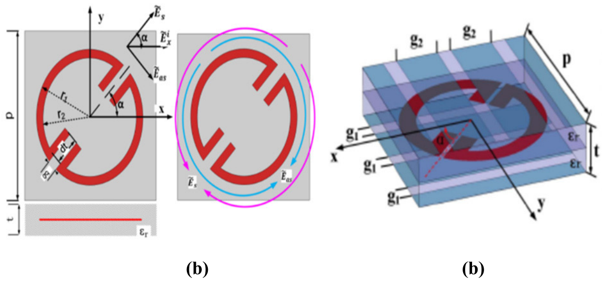

FIGURE 12. **(a) DSRR structure (b) Schematic of the proposed metasurface [121].**

A Fabry-Perot-like cavity has been used as the basis for the development of a multifunctional metasurface [122]. This layout provides control over directions and polarization of incident light in either reflection and transmission modes. The metasurface contains anisotropic unit cells that utilize a split ring structure oriented at 45 degrees as well as two orthogonal metallic gratings shown below in figure 13. The transmitted and reflected phases and amplitudes can be independently controlled using this configuration. The reflection and transmission coefficients for various polarizations, which provide asymmetric transmission are represented as Jones matrices.

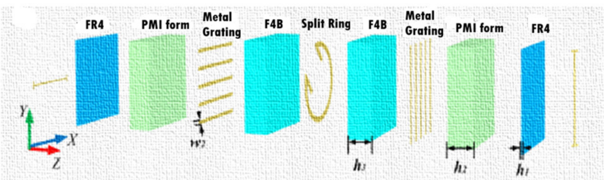

FIGURE 13. **The overall structure of the multilayer unit cell [122].**

4) POLARIZATION DEPENDENT MULTIFUNCTIONAL METASURFACE

The polarization of electromagnetic waves is vital wave propagation, and has garnered increasing interest, particularly in designing compact and multifunctional Metasurfaces.

A typical metasurface for transmissive polarization conversion is designed without a metallic backplate accompanied with a metallic pattern and a dielectric layer. As a result, almost all of electromagnetic waves pass through or rather are transmitted through the metasurface, with a near zero reflection coefficients. The polarization conversion occurs based on the interaction of the incoming wave with the metallic pattern.

For a reflective metasurface, the unit cell for polarization conversion metasurface comprises a patterned layer, a dielectric layer, and a metallic backplate. The backplate hinders the passage of electromagnetic waves. Which as a result, allows most of the incident wave to be reflected with different polarization. Similarly, the polarization conversion happens due to the interactions of the incident waves with the metallic pattern. Han et al. [123] developed an enhanced metasurface to attain polarization conversion within the 8 – 18.9 GHz spectrum. Additionally, Li et al. [124] proposed a double band cross polarization conversion unit across 10.36 and 11.62 GHz frequency respectively. Similarly, Ruan et al. [125] introduced a double band ultra-thin metasurface polarization conversion unit operating within (15.25 – 18.9 GHz) and (29.7 – 36.7 GHz) frequency ranges. Furthermore, Fahad et al. [126] designed a broadband polarization converter functioning within the frequency range of 0.94 to 1.47 THz. A polarization converter with multiple layers in [127] is utilized to produce a tri-band metamaterial. In [128] the authors employed a 2-bit coding structure to manipulate the reflected waves at 7.5 and 13 GHz, thereby achieving a robust meta-hologram with four channels. Nonetheless, most of the work undertaken on polarization conversion before the advent of phase changing materials [129] were solely accomplished on either reflection or transmission. An important aspect of phase-transition materials is the possible advantages from metal-insulator transitions. Jiang et al. [130] presents a vanadium dioxide layer combined with three metal gratings to build a switch that performs the polarization conversion. When the vanadium dioxide acts as a metal, reflection will occur, whereas in the insulator state there is transmission conversion. This method relies on properties of the material to produce adjustable polarization conversion. Hence, it is difficult to achieve effective simultaneous transmission and reflection in one structure that also has polarization conversion.

5) CODING METASURFACES

In 2014, Cui et al. [131] introduced the concept of coding metasurfaces, primarily operating at microwave frequencies. The discrete elements provide distinct phase responses; for instance, the cell 0 and 1 represent phase shifts of 0 and π, respectively, which consists of coding units configured in distinct numerical sequences. The coding metasurface creates a bridge between the analog and digital world through the discretization of the phases. An illustration of a proposed 1-bit coding metasurface and a unit cell structure is shown in figure 14. The geometric design and order of spatial arrangement of these meta-atoms or cells can be designed with high precision based on the phase distribution, which can be used to manipulate of electromagnetic waves to realize several functionalities. The capacity to simultaneously transmit and reflect waves represents a very innovative application of this technology, offering multifunctionality within a single device. This capability is crucial for advanced technologies such as 5G and 6G communication systems, where wavefront management is vital for enhancing network performance.

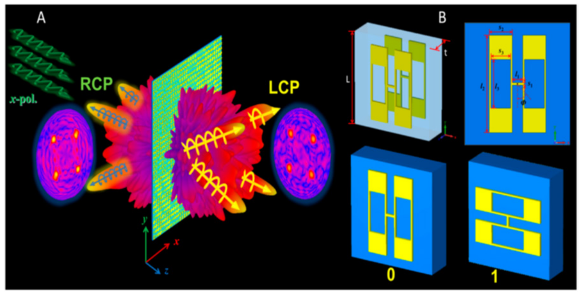

FIGURE 14. Proposed 1-bit coding metasurface and a unit cell structure. (a) multi-function of RCP beams in reflection and LCP beams in transmission. (b) front views of the proposed unit cell [132].

A Fabry-Perot-like cavity metasurface was presented in [122] where the incident wave are manipulated for both transmission and reflection simultaneously but at different frequencies and polarization states. The Fabry-Perot-like cavity enhances the manipulation of phase and amplitude for efficient performance of reflection and transmission, exhibits co-polarized reflection at 21 GHz and cross-polarized transmission at 16 GHz, possesses asymmetric transmission characteristics, and broadband capabilities. The authors in [133] designed a tri-layer dual band coding metasurface with a very low interference for polarization states and different frequency bands. The metasurface operates in dual band, K-band (16GHz to 24GHz) and the Ka-band (37.5GHz to 40GHz) with independent space manipulation and control over the transmission and reflection in these frequency ranges. The tri-layered structure achieves minimal interference between co-polarized reflection and cross-polarized transmission, thereby leading to high efficiency polarization conversion across a broad bandwidth as seen in the performance of the metasurface while maintaining polarization dependent control of incident waves. Coding metasurfaces can be controlled by different characteristics of EM waves, for example in [134] the polarization states of incident waves are altered to achieve transmission and reflection functions at different frequencies. A filter layer is inserted between the transmission and reflection layer to ensure optimal performance in both reflected and transmitted mode. Although, it does not support simultaneous transmission and reflection at the same frequency but allows independent full space manipulation of the waves. A single layer transmission/reflection integrated (TRI) metasurface was proposed in [135], the multi-layered anisotropic structure can transmit and reflect simultaneously at the same frequency 15GHz due to the change in the direction of the incident wave and polarization. When the incident wave is at a 45° along the x-axis, the metasurface can work in reflective and transmissive mode simultaneously at the same frequency, thereby generating two functionalities on both sides of the metasurface. To obtain more degrees of freedom, thermally switchable coding metasurface was proposed in [136], the properties of phase changing materials vanadium dioxide (VO_2) and Indium antimonide (InSb) were utilized as depicted in the fabrication process in figure 15 for the realization of switchable bidirectional metasurface. These two materials exhibit different temperature-dependent properties, the transmission mode operates at lower temperatures (290 K to 330 K), while reflection mode is activated at higher temperature of 370 K, it reflects at one frequency when the material is in a metallic state and transmits at another when in a dielectric state, the transmission and the reflection mode wavefront can be independently manipulated by the phase transition of VO_2 while, InSb is used for frequency switching and the increasing the working bandwidth. Although the metasurface shows effective dual-mode performance but, the transmission bandwidth is narrower than the reflection bandwidth.

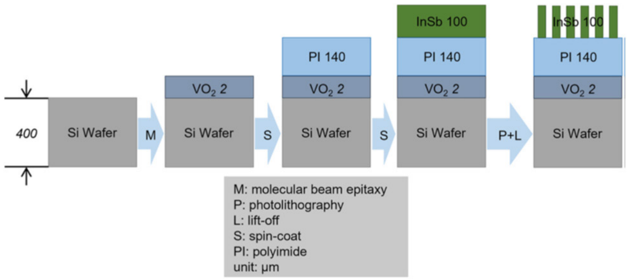

FIGURE 15. Fabrication processes of the metasurface [136].

Dual circular polarization coding metasurface was presented in [132], it ensures minimal interference between the two modes with a phase difference of 180^0 between transmission and reflection. The elements arranged on the metasurface are rotated to control phase which generates four distinct beams for the left circularly polarized (LCP) transmissive waves and right circularly polarized (RCP) reflective waves. The transmission and reflection happen for different polarizations, not the same one. Thus, it does not transmit and reflect the same wave at the same frequency in the same polarization.

A dual-band coding metasurface capable of independent electromagnetic wave control in both the X band and Ku band was presented in [137], the metasurface achieves independent control of transmission and reflection in two frequency bands, operating efficiently and demonstrating high efficiency in both bands. The unit cells are designed to independently manipulate phase and polarization in the two bands without crosstalk, although the design is limited by polarization crosstalk, especially at higher frequencies where the reflection phases are difficult to independently control. Transmission and reflection occur at separate frequencies. The digital coding of the elements is listed in Table 3 to provide a concise design chart. It demonstrates that under x or y polarized excitation, we obtain a 2-bit co-polarized and 1-bit cross-polarized phases; also, under u or v polarized excitation (± 45°-polarized), we obtain 2-bit co-polarized and 1-bit co-polarized phases.

TABLE 3. Coding elements for multifunctional ms.

Output/Input	x(y)-Pol.	X(y)-Pol.	± 45°-Pol.	± 45°-Pol.
(l, φ)/(mm, deg)	X-band (Co-pol.)	Ku-band (Cross-pol.)	X-band (Co-pol.)	Ku-band (Co-pol.)
(10.5, −45)	**00** (0°)	**0** (0°)	**00** (0°)	**0** (0°)
(8.9, −45)	**01** (90°)	**0** (0°)	**01** (90°)	**0** (0°)
(8.2, −45)	**10** (180°)	**0** (0°)	**10** (180°)	**0** (0°)
(6.5, −45)	**11** (270°)	**0** (0°)	**11** (270°)	**0** (0°)
(10.5, 45)	**00** (0°)	**1** (180°)	**00** (0°)	**1** (180°)
(8.9, 45)	**01** (90°)	**1** (180°)	**01** (90°)	**1** (180°)
(8.2, 45)	**10** (180°)	**1** (180°)	**10** (180°)	**1** (180°)
(6.5, 45)	**11** (270°)	**1** (180°)	**11** (270°)	**1** (180°)

In coding metasurfaces, finite phase quantization and non-ideal amplitude control impairs the beamforming gain and spatial multiplexing capacity, which decreases the spectral efficiency capability compared to ideal continuous-phase models. Angular sensitivity also affects the coverage probability where users with oblique incidence have lesser effective aperture and channel reconfiguration. Additionally, dynamic reconfigurations need to be re-estimated by estimation and calibration of the channels and surfaces on a regular basis, increasing the overheads in dynamic setups. These are some limitations to the performance gains in real world systems and the gains in spectral efficiency or coverage is achieved at a cost in terms of increasing the complexity of the hardware and the cost of the system itself.

6) SIMULTANEOUSLY TRANSMITTING AND REFLECTING RECONFIGURABLE INTELLIGENT SURFACES (STAR RIS)

A reconfigurable intelligent surface (RIS) is a two-dimensional (2D) structure that incorporates numerous low cost passive components. In contrast to traditional metasurfaces, a smart controller is integrated with the RIS, allowing for the modulation of wireless signal propagation impinge on the RIS due to the tuned phase response. Additionally, traditional relay systems and multi-antennas actively generate signals using expensive radio frequency chains, whereas Reconfigurable Intelligent Surfaces (RISs) merely passively recycle existing signals in the network and do not necessitate RF chains. Consequently, RISs are less expensive and environmentally sustainable compared to the old antenna systems.

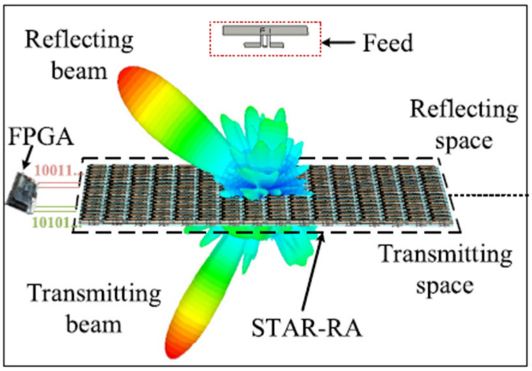

FIGURE 16. Concept of STAR-RA [138].

STAR-RIS uses the concept of reconfiguring of unit cells to control the electromagnetic wave properties (amplitude, phase, or polarization) in both directions, the key feature of STAR-RIS is its ability to split energy between transmission and reflection efficiently in a typical STAR-RIS configuration, the incident signals are separated into two (transmitting and reflecting) signals to facilitate a full-space manipulation by passing into both sides of the spaces. STAR-RISs are capable of transmitting and reflecting the incident signals simultaneously, covering both spaces, thereby serving the half-spaces with a single design as captured in figure 16. For instance, in [7] the properties of incident wave are adjusted to control the transmitted and reflected signals simultaneously. Three (3) operating modes were compared by the authors energy splitting ES, Mode switching MS, and Time switching TS in a unicast and multicast scenario, it was asserted that TS is advantageous for unicast communication due to its low interference, ES is more suited for multicast scenarios due to its full utilization of time and resources. for high quality of service (QoS) requirements, especially in multicast communication, TS is less efficient because it does not fully utilize the available communication time and MS is a simpler approach with less flexibility and gain compared to ES. Similarly, as captured in [139] the transmission and reflection coefficients can be changed by varying electric and magnetic currents of the STAR-RIS elements. consequently, a highly dynamic full-space manipulation can be realized. Despite the advantages stated above, research on the integration of how STAR-RISs can be into wireless communication systems is still in its infancy. Energy splitting and mode switching schemes are used in STAR-RIS to determine the signal-to-interference plus noise ratio (SINR) of users on opposite sides of the surface, therefore, affecting sum-rate and performance. The design made at EM levels, create some fundamental limitations to communication performance that highlight the need to co-design metasurface physics with wireless system goals. The more elements that are controllable, the more power consumption, latency, and reliability issues that come up with biasing networks and digital controllers. In STAR-RIS, simultaneous transmission and reflection makes switching architecture more challenging and reduces fabrication tolerances.

Though the reviewed approaches are different in structural implementation, the relative performance can simply be explained in terms of the mechanism applied to regulate the phase and impedance of the transmission and reflection channel. Huygens metasurfaces provides a wavefront control by balancing both the electric and magnetic responses, and this has demonstrated high efficiency and an almost perfect impedance match, but at a restricted frequency range, limiting the operation to the broadband. Pancharatnam Berry (PB) phase designs, are based on geometrical accumulation of phases with rotation of elements, which enables full coverage of phases, which are largely independent of frequency, yet their work is necessarily conditioned by the polarization conversion efficiency that may limit uniformity of amplitude when reflection and transmission efficiencies are both required to be high. Metasurfaces based on Fabry Perot cavity introduce more longitudinal resonances, making them have more bandwidth and efficiency through controlled multi-path interference This however, leads to increased thickness, sensitivity to loss, and complexity of fabrication. Coding metasurfaces are based on digital phase states and programmability, allowing them to operate multifunctionally and reconfigurably, however quantization and switching tend to negatively affect efficiency and introduce dispersion over large bandwidths. Lastly, STAR-RIS architectures take the simultaneous reflection and transmission beyond a system level paradigm where energy separation and switching of the mode allows adaptive network control, but the practical implementation of these systems is currently restricted by the complexity of hardware and immature implementations. As a result, there is no single strategy that is perfect in all cases, but rather, all strategies would be better than the other subject to certain limitations based on bandwidth, polarization, efficiency, structural and system level complexity.

B. DESIGN PARAMETERS AND METRICS

Figure 17 above outlines key design parameters that defines the behaviour and performance of metasurfaces. Wavefronts can be manipulated by modifying the phase of the incident waves on each meta atom, and thereby enabling beam steering and focusing schemes, which are important in modern communication systems [140], [141], [142]. In addition to phase, amplitude modulation provides another means to adjust the intensity of transmitted or reflected waves, which determines the energy distribution at the wavefront. It is also an important parameter for applications that require signal control over strength [143], [144].

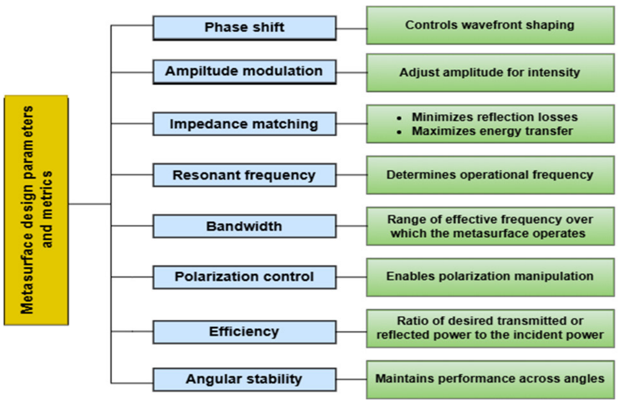

FIGURE 17. Metasurface design parameters and metrics.

Impedance matching [145], on the other hand limits reflection losses in order to maximize power transmissivity. Impedance matching constitutes the hallmark feature of major operations such as transmitarray antennas, since sufficient power testing will not yield good results [146]. The resonances of meta atoms delineate the usable frequency band of the metasurface [147], putting constraints on their viability and considerations for some applications such as terahertz phase modulation [148]. Broad bandwidth encompasses greater effective operation range [149], [150], thus enabling a metasurface to operate in multiple frequency bands, leading to a broadened application horizon such as in multiband communication systems [151], [152].

Advanced functionalities are achieved through polarization control [153], wherein metasurfaces may establish, alter, and manipulate the polarization state of incoming waves. These functionalities are quintessential to several applications that involve the conversion or operation of surface waves, such as polarization conversion or producing circular polarization, as has been proven in several studies [53], [154], [155], [156]. An overall performance metric of a metasurface is its efficiency, it is measured as power transmitted or reflected divided by incident power. An efficiency close to one indicates a good standard in any design and fabrication [157], [158]. The angular stability [159], [160], [161] of a metasurface indicates its capability to work efficiently at different incidence angles which has a special significance for near-field passive mm-wave imaging [162].

The specifications identified will influence the design and optimization techniques for the metasurfaces and assist engineers in formulating the desired package to fulfil the necessary operational requirements and application demands.

In addition to the above design parameters and metrics, surface current density cannot be overlooked in the design of a metasurface. The reflection and transmission properties of a metasurface are determined at a physical level by the spatial distribution of the induced surface current density on the unit cell elements. The magnitude and phase of the reflected and transmitted waves are directly proportional to the strength, orientation, and symmetry of these currents, which can radiate either to the incident half-space, the transmission half-space or both. Designs that support reflection and transmission simultaneously are usually engineered based on many current components such as simultaneous electric and magnetic currents on the surface or polarization dependant current paths to allow enough degrees of freedom to be independently controlled. Consequently, most of the strategies discussed in this paper such as impedance matched designs, multi-resonant structures and polarization based designs could be viewed as various ways of shaping the distributions of surface currents to attain the desirable scattering characteristics. A typical example is in [107] where the authors investigate the resonance mechanism of the unit cell in figure 18.

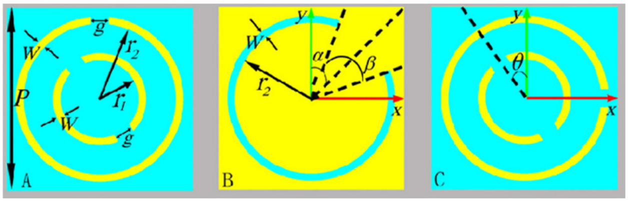

FIGURE 18. The schematic diagram of a full space metasurface. A view of the Tri-layered structure, where (A-C) correspond to the front, middle and back layer of the structure [107].

The induced surface current distributions on the resonator elements of layers A, B, and C are examined for a y-polarized incident wave at 0.55 THz and a left-hand circularly polarized (LCP) wave at 1.37 THz propagating along the -z axis. At 0.55 THz, as shown in Figure. 19(a–c), the induced currents are predominantly concentrated on the outer SSR elements of layers A and B, as well as along the edges of the C-shaped slot resonator in layer B.

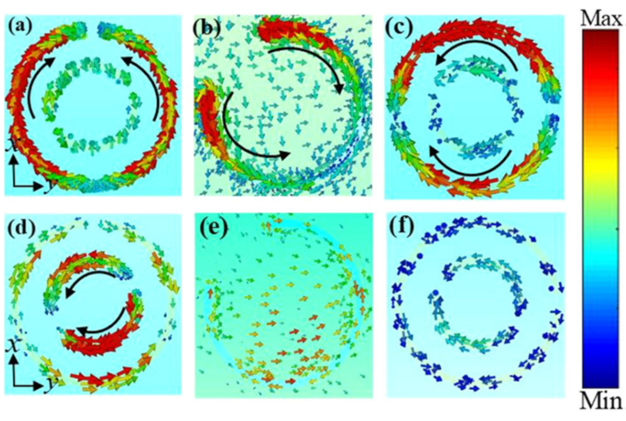

FIGURE 19. The surface current distribution on the structure and the corresponding layers A (a, d), B (b, e) and C (c, f) under y-polarized and LCP waves along-z axis [107].

At higher frequency of 1.37 THz, Figure. 19(d-f) indicate that the induced currents are largely concentrated on the inner structures of layer A and the C-shaped slot resonator of layer B. The opposite current directions in layers A and B represent the magnetic resonance, and in this situation, the conversion of circular polarization on the higher frequency is carried out by the magnetic resonance. The weak coupling and interaction of the inner ring and the C-slot structure allow independent linear-polarized transmission and reflection phase of the circular-polarized by rotation of the inner ring and changing the geometrical parameters of the C-shaped slot resonator.

A comparison of various metasurface design strategies for simultaneous reflection and transmission depicted in Table 4 provides ample diversity in performances that fit different working requirements. The analysis of bandwidth, efficiency, polarization, frequency, and angular stability provides a good basis to differentiate the advantages and disadvantages of these designs as well as their potential improvements. A strong point where a few designs stand head and shoulders above others is bandwidth. The PB Berry metasurface boasts about 112% fractional bandwidth from 9.3 GHz to 32.5 GHz, making it a good candidate for ultra-wideband applications, where wide frequency coverage is an obligation. In stark contrast, a few others worked on STAR-RIS, which operates within a bandwidth of only about 10% (5.7-6.3 GHz), designed for a more focused application, such as that used for 5G communications. Many of the synthesized designs did not report the bandwidth associated with their designs. This may reflect poor reporting on their part, or minimal emphasis is given to bandwidth optimization. Accurate assessment for wideband applications may be difficult without definitive bandwidth performance. The performance of a metasurface is measured primarily through its efficiency. Consistently, Fabry-Perot metasurfaces and some polarization converters have 90% efficiency, indicating minimum insertion losses and high performance. conversely, PB has an efficiency of about 25% but provide exceptionally wide bandwidth. Some designs do not provide enough data which could hinder their usage in applications that require energy efficient system. Furthermore, polarization adds a level of uniqueness to metasurfaces. Linear polarization (LP) remains superior in terms of compatibility with modern systems and simplicity of operation. However, PB and some coding designs can provide dual polarization (LP and CP), exponentially improving their functionality and versatility. For example, polarization conversion metasurfaces operate in both linear-to-linear (LL) and linear-to-circular (LC) modes to support terahertz prospects, where advanced polarization control is required. These metasurfaces have so far covered the traditional GHz to terahertz bands, indicating their diversity in various application. STAR-RIS has a range of use in the mid-range GHz frequency bands (5.7 to 6.3 GHz), while showing robustness for an application space around the communication system proposed for a contemporary wireless system. Performance in real life scenarios requires angular stability but is poorly addressed. The STAR-RIS, for example, shows angular stability at oblique angles up to 30° in a controlled environment, whereas many other designs did not state angular stability in their characterization. Failure to perform such characterization calls for further research, because angular stability is a crucial parameter for metasurface design deployed in multi-user environments.

The comparative analysis of various metasurface designs demonstrates their respective advantages and limitations against one another. While PB metasurfaces are excellent for their bandwidth, they lag in efficiency. STAR-RIS thus provides a middle ground with fair efficiency, single frequency function, and angular stability, to cater for numerous applications like 5G. Nevertheless, not reported "NR" entries of various parameters indicate reporting and characterization gaps that provide further spaces for evaluation. This is mainly because of disparities on design goals and evaluation techniques used in the different studies. A number of papers focus on proof-of-concept demonstrations, with the emphasis on phase manipulation or operating functionality at one frequency and at normal incidence, but with no further analysis of broadband or angular behavior. Elsewhere, the scope of reported results is limited by numerical or experimental constraints, e.g., by limited simulation bandwidth, fixed-angle measurement configurations, or application specific optimization goals. This leads to the fact that not all entries can be compared directly and quantitatively. This brings out the fact that more consistent reporting practices are necessary in the future research. Future advancements in metasurface technology should focus on widening the frequency response, angular stability, and efficiency in order to let metasurfaces exploit their full potential in next-generation communication systems.

IV. RESEARCH CHALLENGES, POTENTIAL SOLUTIONS, AND FUTURE DIRECTIONS

A. FULL SPACE MANIPULATIONS

The manipulation of electromagnetic (EM) waves in full-space is receiving considerable attention, primarily because of its benefits in terms of variable EM responses and the ability to manage multifunctional wave fronts. Reflective or transparent Metasurfaces can control EM waves in half-space through reflection or transmission, leaving the other half-space unused [174], [175], [176]. Full space control of electromagnetic waves involves the simultaneous and independent manipulation of both the reflected and transmitted waves. This allows for the simultaneous and independent control of radiations in both directions.

Several techniques have been reported in the literatures to realise full space manipulations such as decoupling spin channels [119], amplitude and phase control [177], [178], [179], double split ring resonator (DSSR) [121], polarization state [7], [180], digital coding [9], etc. The engineered metasurfaces make use of multilayer structures that enable precise control of EM waves from both directions. This innovation significantly increased information capacity and extended the range of the signal, which is of tremendous value for advanced communication systems. Nevertheless, the presence of amplitude fluctuation in meta-atoms caused

TABLE 4. Comparison of various simultaneous reflection and transmission design strategies.

Design Feature	Operation	Bandwidth	Efficiency	Polarization	Frequency	Angular stability	Ref	Design Limitations
Huygen metasurface	Reflection & transmission	NR	NA	LP	2 to 5GHz	60^0	[109] 2019	Resonance limited bandwidth -Electric–magnetic balance sensitivity -Moderate fabrication complexity
	Reflection & transmission	NR	>80%	LP	11 & 16GHz	NR	[111] 2023	
	Reflection & transmission	13% Relative BW	NR	LP	30GHz	0^0	[115] 2023	
	Reflection & transmission	NR	≈60%	LP	0.83THz	NR	[114] 2024	
PB Berry	Reflection & transmission	52%	≈90%	LP & CP	5.9 to 15.7 GHz	NR	[118] 2019	Polarization dependent -Cross-polarization efficiency limit -Often narrowband when hybridized
	Reflection & transmission	112% Fractional BW	≈25%	CP	9.3 to 32.5 GHz	NR	[116] 2020	
	Reflection & transmission	NR	>90%	LP	12GHz & 18GHz	0^0	[117] 2022	
	Reflection & transmission	NR	>78%	CP	28–30 GHz	Up to 40^0	[119] 2024	
	Reflection & transmission	NR	NR	CP	9GHz	0^0	[163] 2025	
Fabry Perot	Reflection & transmission	NR	90%	LP	18-26GHz	NR	[122] 2019	Cavity resonance, narrowband -Angular sensitivity -Increased thickness
	Reflection & transmission	NR	>90%	LP	23 to 37 GHz	NR	[121] 2022	
	Reflection & transmission	NR	NR	LP	0.9 to 1.2 THz	NR	[164] 2023	
	Reflection & transmission	13.4% Fractional BW	NR	Dual	34 to 40 GHz	Up to 40^0	[165] 2024	
	Reflection & transmission	NR	80%	LP	0.7 to 1.0 THz	NR	[158] 2024	
	Reflection & transmission	NR	88.7%	LP	15GHz	18.2^0	[135] 2018	Phase quantization error -Biasing network
	Reflection & transmission	NR	90%	LP & CP	9 to 14GHz	NR	[134] 2021	

TABLE 4. *(Continued.)* **Comparison of various simultaneous reflection and transmission design strategies.**

Coding Metasurface	Reflection & transmission	NR	80%	LP	10GHz	NR	[166] 2023	complexity -Increased power consumption
	Reflection & transmission	NR	NR	CP	1 to 5GHz	Up to 24^0	[136] 2024	
	Reflection & transmission	NR	NR	LP	0.5-0.9THz	0^0	[167] 2025	
Polarization conversion	Reflection & transmission	NR	90%	LL & LC	4.62-13.56GHz	NR	[168] 2019	Multi-layer structural complexity -Fabrication tolerance sensitivity -Limited broadband decoupling
	Reflection & transmission	NR	≈80%	LL & LC	0.5 to 1.4THz	NR	[107] 2022	
	Reflection & transmission	≈37%	NR	LL & LC	2 to 5GHz	NR	[169] 2023	
	Reflection & transmission	NR	≈70%	LL	7 to 17GHz	NR	[170] 2024	
STAR RIS	Reflection & transmission	NR	NR	LP	NR	NR	[171] 2021	Power splitting constraint -Control circuitry overhead -Calibration complexity
	Reflection & transmission	≈10%	≈68%	LP	5.7–6.3 GHz	30^0	[138] 2023	
	Reflection & transmission	NR	NR	LP	NR	NR	[172] 2024	
	Reflection & transmission	≈28%	NR	LP	26GHz	R_x up to 45^0 T_x up to 30^0	[173] 2025	

by the intricate phase modulation scheme continues to be a topic of concern for future research [119]. Various MSs have been proposed to allow manipulation of EM waves in half or full space [108], [118], [134], [181], [182]. However, they are unable to simultaneously and independently manipulate both reflection and transmission under the same incident wave. The authors' in [168] proposed a multifunctional reconfigurable metasurface that can transmit and reflect but not simultaneously, although it can control the propagation and conversion mode simultaneously. Similarly, in [181] the structure can either transmit or reflect non simultaneously a linearly polarized (LP) incident wave. However, different parameters factor in to independently manipulate the phase of either the transmitted or reflected wave

Open Issues and Future Directions:

a. In order to achieve simultaneous control of phase and amplitude intricate designs, often involving complex geometric or multi-layered structures are required. Optimal phase and amplitude control often leads to efficiency trade-offs, where optimizing one parameter invariably impacts the other.

b. One important issue influencing the effectiveness of full-space manipulation in metasurfaces is bandwidth.

Metasurface's adaptability is limited by narrow bandwidths to certain frequencies, larger bandwidth allows the metasurface to be more versatile and dependable in manipulating waves. Precise control of both transmission and reflection modes becomes somewhat difficult with wideband structure.

c. Angular stability is an essential feature in manipulating waves in full-space and ensures consistent control of electromagnetic waves for normal and oblique angles of incidence. If a metasurface lacks angular stability, the performance of the metasurface could deteriorate at certain angles, resulting in poor manipulation of the wave and loss of phase or amplitude control.

B. ANGULAR STABILITY

The response of a metasurface is carefully assessed based on its angular stability performance. Angular stability is the ability of a metasurface to maintain its intended transmission and reflection responses over a range of angle of incidence without significant degradation in efficiency or phase control. The response of metasurfaces is typically required to be independent of the angle of incidence of the electromagnetic wave in almost all applications. Metasurfaces with angular stability are important for applications where the electromagnetic waves may not be exactly aligned at normal incidence. Such as antenna systems, sensors, and other optical devices. Metasurfaces with angular stability can work efficiently at certain oblique angles across frequency bands while maintaining their performance. An oblique angle of incidence up to 45^0 was reported in [183], it also performs polarization conversion (co and cross) at different frequency band with high efficiency. Similarly, an oblique incident with an angle of 40^0 was presented in [119] with full space manipulation achieved using space spin-decoupled channels. A metasurface's angular stability allows it to perform well in wave manipulation and polarization conversion throughout a large incidence angle range. High angular stability means the metasurface can control electromagnetic waves from multiple directions. To determine angular stability the polarization conversion ratio (PCR) is commonly used. A high PCR, usually above 90%, often translate to a stable metasurface even when the angle of incidence increases, ensuring successful polarization conversion across all angles. Authors in [121], [182], and [183] reported to have a high efficiency of greater than 90% PCR, for both transmission and reflection respectively.

Open Issues and Future Directions:

a. Metasurface with single polarization control tend to have certain performance degradation with respect to angular stability. For example, the limitation in [121] is that the metasurface can only process on type of polarization (LP) and the polarization has to be perpendicular on the two sides

b. Certain operations at higher oblique angle of incidence may result in reduced bandwidth. Mostly there is a trade-off between angular stability and bandwidth operation. Designs with narrow bandwidth operating in both reflection and transmission simultaneously have been reported in [7], [177], and [178]

c. Multi-objective optimization that is assisted by machine learning can help in the simultaneous optimization of phase linearity and angular tolerance.

C. BANDWIDTH PERFORMANCE

Over the years several efforts have been made to increase the efficiency and bandwidth of metasurfaces. Conventional Huygens' principle [108] involves the utilization of balanced electric and magnetic resonances in transverse direction, another approach is the Pancharatnam Berry phase principle [116], [118] where phase control is achieved to enhance the efficiency and bandwidth based on the azimuthal rotation of the subwavelength scatterer which exudes some degree of freedom. Bandwidth is greatly influenced by factors such as element design, material properties and phase control. The orientation, size and shape of Metasurfaces element determine the bandwidth and resonant frequencies, for example, to broaden the operational bandwidth multiple resonant elements can be incorporated, complex designs can limit bandwidth, so also achieving simultaneous transmission and reflection with independent phase control requires complex designs. However, cascaded metasurface have shown promising results in mitigating these limitations. To independently manipulate the transmitted and reflected wave the cascaded Metasurfaces integrate resonant and geometric phase cells [184]. A metasurface with reciprocity-protected transmission and diffuse reflection combined in [185] examine the bandwidth performance and demonstrate that arranging each element in a random sequence can result in a wide working bandwidth. In addition, they highlight the need to balance the trade-offs between maintaining a broad bandwidth and achieving optimal efficiency. Furthermore, they emphasize that this trade-off between bandwidth and efficiency can be minimized by optimizing the metasurface element design specifically through careful selection of geometry, material composition, and arrangement strategy.

Open Issues and Future Directions:

a. Designing a metasurface with high efficiency and broad bandwidth plus angular stability is a challenging task. The major drawback is its reduced bandwidth at higher oblique incidence angles.

b. The designs still exhibit low efficiencies due to the unwanted mutual coupling, although there is a significant enhancement in the bandwidth [116].

c. Future studies can examine dispersion engineered meta-atoms, multi-resonant stacking and non-local metasurface designs.

A consistent finding in the literature reviewed is that there are interdependent trade-offs of bandwidth, efficiency and angular stability. Strong resonant coupling or multi-layer interference are often used to achieve designs optimized to work in ultra-wide bandwidth which improves phase coverage, but add to the dielectric and conductive losses, making such designs less efficient. On the other hand,

TABLE 5. Summary of key challenges and future directions.

Key Parameter	Features	Challenges	Future Direction
Full space manipulation	Involves simultaneous manipulation of reflected and transmitted waves, allowing for independent control in both directions.	Complexity in designs, often requiring intricate geometric or multi-layered structures.	Development of simpler designs that can achieve effective full-space manipulation without significant trade-offs in performance.
Angular stability	Essential for maintaining performance across various angles of incidence. High angular stability ensures effective wave manipulation and polarization conversion at oblique angles.	Limited performance at certain angles can lead to ineffective wave manipulation. Trade-offs between angular stability and bandwidth are common.	Focus on achieving high angular stability while maintaining efficiency and bandwidth across a wide range of incident angles.
Bandwidth Performance	Influenced by element design, material properties, and phase control; larger bandwidth increases versatility but can complicate design.	Narrow bandwidths limit usefulness; complex designs may restrict bandwidth while optimizing for reflection and transmission simultaneously.	Exploration of cascaded metasurfaces and innovative designs that balance broad bandwidth with optimal efficiency.

with high-efficiency single-layer metasurfaces, there is typically narrow band operation and poor angular stability with oblique incidence because the phase dispersion is rapid. Symmetric or multilayer designs are used to enhance the stability of angular responses but this tends to add to the overall thickness and sensitivity to fabrication, especially at millimetre-wave frequencies and beyond. Although impedance-matched Huygens metasurfaces partially counteract the losses of efficiency, but there is still a need to balance the electric and magnetic response with a wide band of incidence angles in an efficient manner. These results suggest that optimization of performance of simultaneous reflection-transmission metasurfaces is multi-objective by nature and that any improvement in a single measure is typically at the cost of another, yet it is important to note that application specific design selection is needed.

Table 5 highlights the key challenges and ways forward for metasurface development. It highlights three challenges; full-space manipulations,maintaining angular stability, and bandwidth performance, all of which are necessary for efficient multifunctional designs. Future work can aim to simplify designs without compromising efficiency while maintaining angular stability, and bandwidth performance.

Based on the challenges discussed above, some avenues of open research can be more clearly outlined. One major issue is how the transmission and reflection phase responses can be successfully separated over broad bandwidths without necessarily using very complex structures or multilayer systems. The other significant direction is the design methodology development that is both high in transmission and reflection efficiency in oblique incidence (angular dispersion and impedance mismatch are high). Also, the ability to operate on broadband with the angular stability is yet to be solved, especially in single layered designs. The answers to these queries require unit cell design, dispersion engineering and systematic optimization frameworks, which considers bandwidth, efficiency, and angular response jointly, rather than treating them independently.

V. CONCLUSION

This paper has presented an extensive review on metasurfaces, specifically the design and realization of structures that can reflect and transmit electromagnetic waves simultaneously. Whereas traditional metasurfaces have primarily been used to control wavefronts through either reflection or transmission, the unidirectional nature of these operations limits usability in scenarios that require full-space manipulation. The review examines the fundamental principles of electromagnetic waves, structural classifications, and performance considerations for reflective and transmissive metasurfaces and how the two functionalities can be merged either in hybrid or cascaded configurations to improve coverage and reconfigurability. Nonetheless, realizing independent control phase and amplitude in both directions poses considerable challenge in design and fabrication. The use of complex unit cell geometries, the need for symmetry-breaking, and the electric and magnetic responses will incur considerable trade-offs between efficiency, bandwidth, angular stability, and polarization control. Numerous strategies for implementing multifunctional metasurfaces were reviewed, such as Pancharatnam Berry phase, Huygens' metasurfaces, multi-resonant and cascaded designs, and anisotropic or active materials. Each of these strategies presents opportunities for decoupling the phase profiles for reflected and transmitted waves, which allows more versatile engineering of the wavefront. For example, both resonant and geometric phase elements can achieve wider operational bandwidth and still maintain independent control of the reflection and transmission channels. Novel design approaches like randomized element arrangements and layered structures were also presented as innovative methods to expand bandwidth and increase angular response, however, this may create additional complexity in fabrication. Metasurfaces capable of simultaneous reflection and transmission offer exciting functional advantages, but the realization of this structures demands several design trade-offs. Achieving high efficiency and broad bandwidth often necessitates more intricate structural designs, which can hinder scalability. However, the studies reviewed in this article show that these challenges can be remedied. With refined unit cell engineering, smart layering arrangements, and the use of tunable or reconfigurable elements, many of the performance constraints can be effectively resolved.

Metasurfaces that support simultaneous reflection and transmission represents a pivotal step towards advancement in electromagnetic wave control. Extending the capabilities of conventional metasurfaces configurations, opens up new modes of wave manipulation. Furthermore, continued advances in design strategies and materials technologies will be essential for unlocking their potential across diverse application.

REFERENCES

[1] A. Alù, M. G. Silveirinha, A. Salandrino, and N. Engheta, "Epsilon-near-zero metamaterials and electromagnetic sources: Tailoring the radiation phase pattern," *Phys. Rev. B, Condens. Matter*, vol. 75, no. 15, Apr. 2007, Art. no. 155410.

[2] H.-T. Chen, W. J. Padilla, J. M. O. Zide, A. C. Gossard, A. J. Taylor, and R. D. Averitt, "Active terahertz metamaterial devices," *Nature*, vol. 444, no. 7119, pp. 597–600, Nov. 2006.

[3] T. Ergin, N. Stenger, P. Brenner, J. B. Pendry, and M. Wegener, "Three-dimensional invisibility cloak at optical wavelengths," *Science*, vol. 328, no. 5976, pp. 337–339, Apr. 2010.

[4] J. B. Pendry, D. Schurig, and D. R. Smith, "Controlling electromagnetic fields," *Science*, vol. 312, no. 5781, pp. 1780–1782, Jun. 2006.

[5] D. Schurig, J. J. Mock, B. J. Justice, S. A. Cummer, J. B. Pendry, A. F. Starr, and D. R. Smith, "Metamaterial electromagnetic cloak at microwave frequencies," *Science*, vol. 314, no. 5801, pp. 977–980, Nov. 2006.

[6] D. R. Smith, J. B. Pendry, and M. C. Wiltshire, "Metamaterials and negative refractive index," *Science*, vol. 305, no. 5685, pp. 788–792, 2004.

[7] Y. Zhuang, G. Wang, T. Cai, and Q. Zhang, "Design of bifunctional metasurface based on independent control of transmission and reflection," *Opt. Exp.*, vol. 26, no. 3, pp. 3594–3603, 2018.

[8] T. H. Nguyen and G. Byun, "A suboptimal approach to Huygens' metasurfaces for wide-angle refraction," *IEEE Trans. Microw. Theory Techn.*, vol. 70, no. 5, pp. 2588–2598, May 2022.

[9] A. Roy, Y. Naresh, A. Padmanabhan, A. Chockalingam, and K. J. Vinoy, "Digitally reconfigurable metasurface array for a multipath based wireless link with media-based modulation," *IEEE Trans. Microw. Theory Techn.*, vol. 70, no. 12, pp. 5418–5426, Dec. 2022.

[10] Y. Wei, J. Duan, H. Jing, Z. Lyu, J. Hao, Z. Qu, J. Wang, and B. Zhang, "A multiband, polarization-controlled metasurface absorber for electromagnetic energy harvesting and wireless power transfer," *IEEE Trans. Microw. Theory Techn.*, vol. 70, no. 5, pp. 2861–2871, May 2022.

[11] H. Xue, X. Wu, X. Cui, M. Chang, H. Liu, L. Li, and T. J. Cui, "Multitarget wireless power transfer system using metasurface for Quasi–Bessel beams with large half power beam length," *IEEE Trans. Microw. Theory Techn.*, vol. 70, no. 10, pp. 4449–4462, Oct. 2022.

[12] K. Zhang, Y. Wang, S. N. Burokur, and Q. Wu, "Generating dual-polarized vortex beam by detour phase: From phase gradient metasurfaces to metagratings," *IEEE Trans. Microw. Theory Techn.*, vol. 70, no. 1, pp. 200–209, Jan. 2022.

[13] H. Shi, R. Liu, Z. Zhang, X. Chen, L. Wang, J. Yi, H. Liu, and A. Zhang, "A dual-polarized reflective reconfigurable metasurface with stable amplitude based on guided-wave-driven structure," *IEEE Antennas Wireless Propag. Lett.*, vol. 23, no. 6, pp. 1720–1724, Jun. 2024.

[14] A. Ali, M. Khalily, D. Serghiou, and R. Tafazolli, "Reflective metasurface with steered OAM beams for THz communications," *IEEE Access*, vol. 11, pp. 12394–12401, 2023.

[15] A. V. Kildishev, A. Boltasseva, and V. M. Shalaev, "Planar photonics with metasurfaces," *Science*, vol. 339, no. 6125, 2013, Art. no. 1232009.

[16] K. Singh, F. Ahmed, and K. Esselle, "Electromagnetic metasurfaces: Insight into evolution, design and applications," *Crystals*, vol. 12, no. 12, p. 1769, Dec. 2022.

[17] N. Chen, S. Yang, and S. An, "A new hybrid algorithm based on PSO and fireworks algorithm for optimal design of metasurface absorber in RF energy harvesting," *IEEE Trans. Magn.*, vol. 61, no. 2, pp. 1–4, Feb. 2025.

[18] S. K. Verma and S. K. Srivastava, "Single step fabricated low cost and flexible Fano resonant all-metal plasmonic metasurface absorber," *IEEE Photon. Technol. Lett.*, vol. 35, no. 17, pp. 923–926, Sep. 2023.

[19] X. Zhang, Y. Gao, W. Hu, and T. Hong, "Directional modulation of scattering patterns based on conformal holographic metasurface," *IEEE Antennas Wireless Propag. Lett.*, vol. 23, no. 11, pp. 3857–3861, Nov. 2024.

[20] M. Qu, K. Zhang, J. Su, Y. Li, L. Deng, and X. Li, "An enhanced diffractive neural network for metasurface holograms with high resolution, low noise, and uniform intensity," *IEEE Trans. Antennas Propag.*, vol. 72, no. 11, pp. 8600–8610, Nov. 2024.

[21] Z. Wei, H. Xue, Y. Li, S. Zhao, Z. Chen, and L. Li, "A hybrid RF and solar integrated energy harvesting system using optically transparent metasurface," *IEEE Trans. Antennas Propag.*, vol. 73, no. 2, pp. 920–927, Feb. 2025.

[22] R. Aneesh Kumar, C. Saha, and R. Sethunadh, "Dual band metasurface integrated with wideband power combiner for RF energy harvesting," *IEEE Microw. Wireless Technol. Lett.*, vol. 33, no. 9, pp. 1377–1380, Sep. 2023.

[23] X. Yang, E. Wen, D. Bharadia, and D. F. Sievenpiper, "Multifunctional metasurface: Simultaneous beam steering, polarization conversion, and phase offset," *IEEE Trans. Antennas Propag.*, vol. 72, no. 5, pp. 4589–4593, May 2024.

[24] N. Pouyanfar, J. Nourinia, C. Ghobadi, and V. Nayyeri, "Low-profile reflective surface for multi-band linear-to-linear and linear-to-circular polarization conversion," *IEEE Access*, vol. 11, pp. 135159–135165, 2023.

[25] M. Magarotto, L. Schenato, M. Santagiustina, A. Galtarossa, and A.-D. Capobianco, "Plasma-based intelligent reflecting surface for beam-steering and polarization conversion," *IEEE Access*, vol. 11, pp. 43546–43556, 2023.

[26] C. H. S. Nkimbeng, H. Wang, D. Yoon, Y. B. Park, H. Han, and I. Park, "Ultra-wideband ultra-thin transmissive linear to circular polarization convertor based on crossed-dipole-shaped metasurface," *IEEE Access*, vol. 12, pp. 120337–120346, 2024.

[27] Y. Jia, H. Lu, Z. Fan, B. Wu, F. Qu, M.-J. Zhao, C. Qian, and H. Chen, "High-efficiency transmissive tunable metasurfaces for binary cascaded diffractive layers," *IEEE Trans. Antennas Propag.*, vol. 72, no. 5, pp. 4532–4540, May 2024.

[28] M. Zhang, P. Dong, Y. Wang, B. Wang, L. Yang, R. Wu, W. Hou, and J. Zhang, "Tunable terahertz wavefront modulation based on phase change materials embedded in metasurface," *Nanomaterials*, vol. 12, no. 20, p. 3592, Oct. 2022.

[29] X. Zhang, H. Zhang, L. Liu, Z. Han, H. V. Poor, and B. Di, "Target detection and positioning aided by reconfigurable surfaces: Reflective or holographic," *IEEE Trans. Wireless Commun.*, vol. 23, no. 12, pp. 19215–19230, Dec. 2024.

[30] Z. Xing, J. Liao, Z. Xu, X. Cheng, and J. Zhang, "The design of highly reflective all-dielectric metasurfaces based on diamond resonators," *Photonics*, vol. 11, no. 11, p. 1015, Oct. 2024.

[31] X. Yuan, Y. J. A. Zhang, Y. Shi, W. Yan, and H. Liu, "Reconfigurable-intelligent-surface empowered wireless communications: Challenges and opportunities," *IEEE Wireless Commun.*, vol. 28, no. 2, pp. 136–143, Feb. 2021.

[32] S. Aboagye, A. R. Ndjiongue, T. M. N. Ngatched, O. A. Dobre, and H. V. Poor, "RIS-assisted visible light communication systems: A tutorial," *IEEE Commun. Surv. Tut.*, vol. 25, no. 1, pp. 251–288, 1st Quart., 2023.

[33] F. C. Okogbaa, Q. Z. Ahmed, F. A. Khan, W. B. Abbas, F. Che, S. A. R. Zaidi, and T. Alade, "Design and application of intelligent reflecting surface (IRS) for beyond 5G wireless networks: A review," *Sensors*, vol. 22, no. 7, p. 2436, 2022.

[34] H. Zhang and B. Di, "Intelligent omni-surfaces: Simultaneous refraction and reflection for full-dimensional wireless communications," *IEEE Commun. Surv. Tut.*, vol. 24, no. 4, pp. 1997–2028, 4th Quart., 2022.

[35] Y. Liu, X. Liu, X. Mu, T. Hou, J. Xu, M. Di Renzo, and N. Al-Dhahir, "Reconfigurable intelligent surfaces: Principles and opportunities," *IEEE Commun. Surv. Tut.*, vol. 23, no. 3, pp. 1546–1577, Mar. 2021.

[36] H. Zhang, S. Zeng, B. Di, Y. Tan, M. Di Renzo, M. Debbah, Z. Han, H. V. Poor, and L. Song, "Intelligent omni-surfaces for full-dimensional wireless communications: Principles, technology, and. implementation," *IEEE Commun. Mag.*, vol. 60, no. 2, pp. 39–45, Feb. 2022.

[37] H. Zhang, B. Di, K. Bian, Z. Han, H. V. Poor, and L. Song, "Toward ubiquitous sensing and localization with reconfigurable intelligent surfaces," in *Proc. IEEE*, Sep. 2022, vol. 110, no. 9, pp. 1401–1422.

[38] E. Björnson, H. Wymeersch, B. Matthiesen, P. Popovski, L. Sanguinetti, and E. De Carvalho, "Reconfigurable intelligent surfaces: A signal processing perspective with wireless applications," *IEEE Signal Process. Mag.*, vol. 39, no. 2, pp. 135–158, Feb. 2022.

[39] Q. Wu, S. Zhang, B. Zheng, C. You, and R. Zhang, "Intelligent reflecting surface-aided wireless communications: A tutorial," *IEEE Trans. Commun.*, vol. 69, no. 5, pp. 3313–3351, May 2021.

[40] S. K. Das, F. Benkhelifa, Y. Sun, H. Abumarshoud, Q. H. Abbasi, M. A. Imran, and L. Mohjazi, "Comprehensive review on ML-based RIS-enhanced IoT systems: Basics, research progress and future challenges," *Comput. Netw.*, vol. 224, Apr. 2023, Art. no. 109581.

[41] B. Rana, S.-S. Cho, and I.-P. Hong, "Review paper on hardware of reconfigurable intelligent surfaces," *IEEE Access*, vol. 11, pp. 29614–29634, 2023.

[42] M. Ahmed, A. Wahid, S. S. Laique, W. U. Khan, A. Ihsan, F. Xu, S. Chatzinotas, and Z. Han, "A survey on STAR-RIS: Use cases, recent advances, and future research challenges," *IEEE Internet Things J.*, vol. 10, no. 16, pp. 14689–14711, Aug. 2023.

[43] M. Ahmed, A. Wahid, W. U. Khan, F. Khan, A. Ihsan, Z. Ali, K. M. Rabie, T. Shongwe, and Z. Han, "A survey on RIS advances in terahertz communications: Emerging paradigms and research frontiers," *IEEE Access*, vol. 12, pp. 173867–173901, 2024.

[44] B. Zheng, C. You, W. Mei, and R. Zhang, "A survey on channel estimation and practical passive beamforming design for intelligent reflecting surface aided wireless communications," *IEEE Commun. Surveys Tuts.*, vol. 24, no. 2, pp. 1035–1071, 2nd Quart., 2022.

[45] K. Achouri and C. Caloz, "Design, concepts, and applications of electromagnetic metasurfaces," *Nanophotonics*, vol. 7, no. 6, pp. 1095–1116, Jun. 2018.

[46] K. Achouri, M. A. Salem, and C. Caloz, "General metasurface synthesis based on susceptibility tensors," *IEEE Trans. Antennas Propag.*, vol. 63, no. 7, pp. 2977–2991, Jul. 2015.

[47] H.-H. Hsiao, C. H. Chu, and D. P. Tsai, "Fundamentals and applications of metasurfaces," *Small Methods*, vol. 1, no. 4, pp. 1–20, Apr. 2017.

[48] L. Zheng and Y. Zhao, "Generalized Snell's law and its verification by metasurface," in *Proc. 14th Int. Conf. Innov. Mobile Internet Services Ubiquitous Comput. Innov. Mobile Internet Services in Ubiquitous Comput.* Cham, Switzerland: Springer, 2021, pp. 364–372.

[49] A. K. Iyer, A. Alù, and A. Epstein, "Metamaterials and metasurfaces—Historical context, recent advances, and future directions," *IEEE Trans. Antennas Propag.*, vol. 68, no. 3, pp. 1223–1231, Mar. 2020.

[50] R. Malleboina, J. C. Dash, A. Lemma, and D. Sarkar, "On the aperture size of digitally coded metasurfaces for beam steering applications using anomalous reflection," in *Proc. Int. Microw. Antenna Symp. (IMAS)*, Feb. 2023, pp. 255–258.

[51] H. Ren, G. Briere, X. Fang, P. Ni, R. Sawant, S. Héron, S. Chenot, S. Vézian, B. Damilano, V. Brändli, S. A. Maier, and P. Genevet, "Metasurface orbital angular momentum holography," *Nature Commun.*, vol. 10, no. 1, p. 2986, Jul. 2019.

[52] E. Isnard, S. Héron, S. Lanteri, and M. Elsawy, "Advancing wavefront shaping with resonant nonlocal metasurfaces: Beyond the limitations of lookup tables," *Sci. Rep.*, vol. 14, no. 1, p. 1555, Jan. 2024.

[53] J. Li, Y. Yuan, Q. Wu, and K. Zhang, "Bi-isotropic Huygens' metasurface for polarization-insensitive cross-polarization conversion and wavefront manipulation," *IEEE Trans. Antennas Propag.*, vol. 72, no. 3, pp. 2445–2454, Mar. 2024.

[54] N. Yu and F. Capasso, "Flat optics with designer metasurfaces," *Nature Mater.*, vol. 13, no. 2, pp. 139–150, Feb. 2014.

[55] N. U. Hassan, J. An, M. Di Renzo, M. Debbah, and C. Yuen, "Efficient beamforming and radiation pattern control using stacked intelligent metasurfaces," *IEEE Open J. Commun. Soc.*, vol. 5, pp. 599–611, 2024.

[56] W. Li, T. Shen, B. Zhang, and Y. Wei, "A scalable, wide-angle metasurface array for electromagnetic energy harvesting," *Micromachines*, vol. 15, no. 7, p. 904, Jul. 2024.

[57] C. L. Holloway, E. F. Kuester, J. A. Gordon, J. O'Hara, J. Booth, and D. R. Smith, "An overview of the theory and applications of metasurfaces: The two-dimensional equivalents of metamaterials," *IEEE Antennas Propag. Mag.*, vol. 54, no. 2, pp. 10–35, Apr. 2012.

[58] A. A. G. Amer, S. Z. Sapuan, N. Nasimuddin, A. Alphones, and N. B. Zinal, "A comprehensive review of metasurface structures suitable for RF energy harvesting," *IEEE Access*, vol. 8, pp. 76433–76452, 2020.

[59] X. Meng, M. Nekovee, and D. Wu, "The design and analysis of electronically reconfigurable liquid crystal-based reflectarray metasurface for 6G beamforming, beamsteering, and beamsplitting," *IEEE Access*, vol. 9, pp. 155564–155575, 2021.

[60] N. Mohammadi Estakhri and A. Alù, "Wave-front transformation with gradient metasurfaces," *Phys. Rev. X*, vol. 6, no. 4, Oct. 2016, Art. no. 041008.

[61] S. Yu, L. Li, G. Shi, C. Zhu, X. Zhou, and Y. Shi, "Design, fabrication, and measurement of reflective metasurface for orbital angular momentum vortex wave in radio frequency domain," *Appl. Phys. Lett.*, vol. 108, no. 12, Mar. 2016, Art. no. 121903.

[62] M. Lee, J. Lee, D. A. Pham, and S. Lim, "Low-cost and purely passive reflective metasurface using modular meta-strip for indoor sub-6-GHz communication," *IEEE Trans. Instrum. Meas.*, vol. 74, pp. 1–9, 2025.

[63] W. U. Khan, E. Lagunas, Z. Ali, M. A. Javed, M. Ahmed, S. Chatzinotas, B. Ottersten, and P. Popovski, "Opportunities for physical layer security in UAV communication enhanced with intelligent reflective surfaces," *IEEE Wireless Commun.*, vol. 29, no. 6, pp. 22–28, Dec. 2022.

[64] S. Chen, C. Lian, J. Yun, D. Yang, and J. Li, "A Huygens metasurface unit design based on rectangular periods," in *Proc. Cross Strait Radio Sci. Wireless Technol. Conf. (CSRSWTC)*, Nov. 2024, pp. 1–3.

[65] K. M. Kossifos, J. Georgiou, and M. A. Antoniades, "ASIC-enabled programmable metasurfaces—Part 1: Design and characterization," *IEEE Trans. Antennas Propag.*, vol. 72, no. 3, pp. 2790–2799, Mar. 2024.

[66] H. Zhou, X. Yu, P. Wang, Y. Wang, and Z. Yan, "Wideband linear-to-multi-polarization converter based on active metasurface," *IEEE Trans. Antennas Propag.*, vol. 71, no. 6, pp. 5246–5255, Jun. 2023.

[67] M. Najafi, V. Jamali, R. Schober, and H. V. Poor, "Physics-based modeling and scalable optimization of large intelligent reflecting surfaces," *IEEE Trans. Commun.*, vol. 69, no. 4, pp. 2673–2691, Apr. 2021.

[68] S. Y. Wang, Q. W. Zhang, X. H. Zhang, and Y. B. Li, "The design of wideband nonreciprocal transmission by active metasurface," *IEEE Antennas Wireless Propag. Lett.*, vol. 22, pp. 2012–2016, 2023.

[69] J. Tang, S. Xu, F. Yang, and M. Li, "Recent developments of transmissive reconfigurable intelligent surfaces reconfigurable intelligent surfaces: A review," *ZTE Commun.*, vol. 20, no. 1, p. 21, 2022.

[70] Q. Wu and R. Zhang, "Intelligent reflecting surface enhanced wireless network via joint active and passive beamforming," *IEEE Trans. Wireless Commun.*, vol. 18, no. 11, pp. 5394–5409, Nov. 2019.

[71] W. U. Khan, A. Mahmood, A. Bozorgchenani, M. A. Jamshed, A. Ranjha, E. Lagunas, H. Pervaiz, S. Chatzinotas, B. Ottersten, and P. Popovski, "Opportunities for intelligent reflecting surfaces in 6G empowered V2X communications," *IEEE Internet Things Mag.*, vol. 7, no. 6, pp. 72–79, Nov. 2024.

[72] C. Niu, M. Phaneuf, and P. Mojabi, "Transmissive metasurface synthesis from far-field masks using unsupervised learning," *IEEE Antennas Wireless Propag. Lett.*, vol. 23, pp. 2371–2375, 2024.

[73] E. Basar, "Wireless communications through reconfigurable intelligent surfaces," *IEEE Access*, vol. 7, pp. 116753–116773, 2019.
[74] Z. Zhang, L. Dai, X. Chen, C. Liu, F. Yang, R. Schober, and H. V. Poor, "Active RIS vs. passive RIS: Which will prevail in 6G?" *IEEE Trans. Commun.*, vol. 71, no. 3, pp. 1707–1725, Mar. 2022.
[75] Z. Peng, Z. Zhang, C. Pan, M. D. Renzo, O. A. Dobre, and J. Wang, "Beamforming optimization for active RIS-aided multiuser communications with hardware impairments," *IEEE Trans. Wireless Commun.*, vol. 23, no. 8, pp. 9884–9898, Aug. 2024.
[76] K. Duan, "Low-scattering and dual-polarized reconfigurable reflectarray antenna based on absorptive and active coding metasurfaces," *IEEE Trans. Antennas Propag.*, vol. 72, no. 3, pp. 2490–2501, Mar. 2024.
[77] J. Lončar and Z. Šipuš, "Challenges in design of power-amplifying active metasurfaces," in *Proc. Int. Symp. ELMAR*, Sep. 2020, pp. 9–12.
[78] K.-T. Nguyen, T.-H. Vu, H. Shin, and S. Kim, "Performance analysis of active RIS and passive RIS-aided MISO systems over Nakagami-*m* fading channel with imperfect CSI," *IEEE Trans. Veh. Technol.*, vol. 74, no. 3, pp. 4334–4348, Mar. 2025.
[79] C. Kohlberger, S. Karamzadeh, and A. Stelzer, "Active and passive lenses from coupled square ring slots," *IEEE J. Microw.*, vol. 4, no. 3, pp. 416–427, Jul. 2024.
[80] W. Long, R. Chen, M. Moretti, W. Zhang, and J. Li, "A promising technology for 6G wireless networks: Intelligent reflecting surface," *J. Commun. Inf. Netw.*, vol. 6, no. 1, pp. 1–16, Mar. 2021.
[81] I. Yildirim, F. Kilinc, E. Basar, and G. C. Alexandropoulos, "Hybrid RIS-empowered reflection and decode-and-forward relaying for coverage extension," *IEEE Commun. Lett.*, vol. 25, no. 5, pp. 1692–1696, May 2021.
[82] P. Sakyi, J. Dugan, D. Kundu, T. J. Smy, and S. Gupta, "Waveguide-floquet mapping using surface susceptibilities for passive and active metasurface unit-cell characterization," *IEEE Trans. Antennas Propag.*, vol. 72, no. 9, pp. 7110–7121, Sep. 2024.
[83] W. U. Khan, A. Mahmood, M. A. Jamshed, E. Lagunas, M. Ahmed, and S. Chatzinotas, "Beyond diagonal RIS for 6G non-terrestrial networks: Potentials and challenges," 2024, *arXiv:2406.10691*.
[84] R. Schroeder, J. He, and M. Juntti, "Passive RIS vs. hybrid RIS: A comparative study on channel estimation," in *Proc. IEEE 93rd Vehicular Technol. Conf.*, Jul. 2021, pp. 1–7.
[85] J. Hu, S. Bandyopadhyay, Y.-H. Liu, and L.-Y. Shao, "A review on metasurface: From principle to smart metadevices," *Frontiers Phys.*, vol. 8, pp. 1–20, Jan. 2021.
[86] N. Yu, P. Genevet, M. A. Kats, F. Aieta, J.-P. Tetienne, F. Capasso, and Z. Gaburro, "Light propagation with phase discontinuities: Generalized laws of reflection and refraction," *Science*, vol. 334, no. 6054, pp. 333–337, Oct. 2011.
[87] S. B. Glybovski, S. A. Tretyakov, P. A. Belov, Y. S. Kivshar, and C. R. Simovski, "Metasurfaces: From microwaves to visible," *Phys. Rep.*, vol. 634, pp. 1–72, May 2016.
[88] J. Su, Y. Lu, H. Zhang, Z. Li, Y. Yang, Y. Che, and K. Qi, "Ultra-wideband, wide angle and polarization-insensitive specular reflection reduction by metasurface based on parameter-adjustable meta-atoms," *Sci. Rep.*, vol. 7, no. 1, p. 42283, Feb. 2017.
[89] S.-W. Qu, W.-W. Wu, B.-J. Chen, H. Yi, X. Bai, K. B. Ng, and C. H. Chan, "Controlling dispersion characteristics of terahertz metasurface," *Sci. Rep.*, vol. 5, no. 1, p. 9367, Mar. 2015.
[90] J. Huang, "The development of inflatable array antennas," *IEEE Antennas Propag. Mag.*, vol. 43, no. 4, pp. 44–50, 2001.
[91] R. Anwar, L. Mao, and H. Ning, "Frequency selective surfaces: A review," *Appl. Sci.*, vol. 8, no. 9, p. 1689, Sep. 2018.
[92] M. R. Chaharmir, J. Shaker, and H. Legay, "Broadband design of a single layer large reflectarray using multi cross loop elements," *IEEE Trans. Antennas Propag.*, vol. 57, no. 10, pp. 3363–3366, Oct. 2009.
[93] S.-W. Qu, Q.-Y. Chen, M.-Y. Xia, and X. Y. Zhang, "Single-layer dual-band reflectarray with single linear polarization," *IEEE Trans. Antennas Propag.*, vol. 62, no. 1, pp. 199–205, Jan. 2014.
[94] W. Menzel, M. Al-Tikriti, and R. Leberer, "A 76 GHz multiple-beam planar reflector antenna," in *Proc. 32nd Eur. Microw. Conf.*, Oct. 2002, pp. 1–4.
[95] K. K. Karnati, Y. Yusuf, S. Ebadi, and X. Gong, "Theoretical analysis on reflection properties of reflectarray unit cells using quality factors," *IEEE Trans. Antennas Propag.*, vol. 61, no. 1, pp. 201–210, Jan. 2013.
[96] H. Rajagopalan and Y. Rahmat-Samii, "On the reflection characteristics of a reflectarray element with low-loss and high-loss substrates," *IEEE Antennas Propag. Mag.*, vol. 52, no. 4, pp. 73–89, Aug. 2010.
[97] R. H. Phillion and M. Okoniewski, "Lenses for circular polarization using planar arrays of rotated passive elements," *IEEE Trans. Antennas Propag.*, vol. 59, no. 4, pp. 1217–1227, Apr. 2011.
[98] D. R. Smith, W. J. Padilla, D. C. Vier, S. C. Nemat-Nasser, and S. Schultz, "Composite medium with simultaneously negative permeability and permittivity," *Phys. Rev. Lett.*, vol. 84, no. 18, pp. 4184–4187, May 2000.
[99] T. Driscoll, G. O. Andreev, D. N. Basov, S. Palit, S. Y. Cho, N. M. Jokerst, and D. R. Smith, "Tuned permeability in terahertz split-ring resonators for devices and sensors," *Appl. Phys. Lett.*, vol. 91, no. 6, Aug. 2007, Art. no. 062511.
[100] J. F. O'Hara, R. Singh, I. Brener, E. Smirnova, J. Han, A. J. Taylor, and W. Zhang, "Thin-film sensing with planar terahertz metamaterials: Sensitivity and limitations," *Opt. Exp.*, vol. 16, no. 3, pp. 1786–1795, 2008.
[101] C. Pfeiffer and A. Grbic, "Metamaterial Huygens' surfaces: Tailoring wave fronts with reflectionless sheets," *Phys. Rev. Lett.*, vol. 110, no. 19, May 2013, Art. no. 197401.
[102] C. Pfeiffer, N. K. Emani, A. M. Shaltout, A. Boltasseva, V. M. Shalaev, and A. Grbic, "Efficient light bending with isotropic metamaterial Huygens' surfaces," *Nano Lett.*, vol. 14, no. 5, pp. 2491–2497, May 2014.
[103] S.-W. Qu, H. Yi, B. J. Chen, K. B. Ng, and C. H. Chan, "Terahertz reflecting and transmitting metasurfaces," *Proc. IEEE*, vol. 105, no. 6, pp. 1166–1184, Jun. 2017.
[104] X.-Y. Jiang, J.-S. Ye, J.-W. He, X.-K. Wang, D. Hu, S.-F. Feng, Q. Kan, and Y. Zhang, "An ultrathin terahertz lens with axial long focal depth based on metasurfaces," *Opt. Exp.*, vol. 21, no. 24, pp. 30030–30038, 2013.
[105] M. I. Shalaev, J. Sun, A. Tsukernik, A. Pandey, K. Nikolskiy, and N. M. Litchinitser, "High-efficiency all-dielectric metasurfaces for ultracompact beam manipulation in transmission mode," *Nano Lett.*, vol. 15, no. 9, pp. 6261–6266, 2015.
[106] J. Luo, H. Yu, M. Song, and Z. Zhang, "Highly efficient wavefront manipulation in terahertz based on plasmonic gradient metasurfaces," *Opt. Lett.*, vol. 39, no. 8, pp. 2229–2231, 2014.
[107] J. Li, Y. Cheng, J. Fan, F. Chen, H. Luo, and X. Li, "High-efficiency terahertz full-space metasurface for the transmission linear and reflection circular polarization wavefront manipulation," *Phys. Lett. A*, vol. 428, Mar. 2022, Art. no. 127932.
[108] F. S. Cuesta, I. A. Faniayeu, V. S. Asadchy, and S. A. Tretyakov, "Planar broadband Huygens' metasurfaces for wave manipulations," *IEEE Trans. Antennas Propag.*, vol. 66, no. 12, pp. 7117–7127, Dec. 2018.
[109] Z. Sun, B. Sima, J. Zhao, and Y. Feng, "Electromagnetic polarization conversion based on Huygens' metasurfaces with coupled electric and magnetic resonances," *Opt. Exp.*, vol. 27, no. 8, pp. 11006–11017, 2019.
[110] V. G. Ataloglou, M. Chen, M. Kim, and G. V. Eleftheriades, "Microwave Huygens' metasurfaces: Fundamentals and applications," *IEEE J. Microw.*, vol. 1, no. 1, pp. 374–388, Jan. 2021.
[111] S. Wang, G. Zhai, Y. Chen, J. Gao, Y. Zhou, X. Wang, Z. Zhang, and J. Ren, "Compact dual-band independently modulated Huygens' metasurface for full-space EM wave manipulation," *IEEE Trans. Microwave Theory Techn.*, vol. 71, no. 12, pp. 5160–5170, Nov. 2023.
[112] M. Chen and G. V. Eleftheriades, "Omega-bianisotropic wire-loop Huygens' metasurface for reflectionless wide-angle refraction," *IEEE Trans. Antennas Propag.*, vol. 68, no. 3, pp. 1477–1490, Mar. 2020.
[113] N. Ullah, R. Zhao, and L. Huang, "Recent advancement in optical metasurface: Fundament to application," *Micromachines*, vol. 13, no. 7, p. 1025, 2022.
[114] Y. Li, S. Wan, R. Zhao, Z. Zhu, W. Li, C. Guan, J. Yang, A. Bogdanov, P. Belov, and J. Shi, "Huygens' metasurface: From anomalous refraction to reflection," *Opt. Commun.*, vol. 565, Aug. 2024, Art. no. 130648.
[115] A. Berto, F. F. Manzillo, and G. Valerio, "Analysis of Huygens' metasurfaces for the design of transmit-reflect arrays," in *Proc. 17th Eur. Conf. Antennas Propag. (EuCAP)*, Mar. 2023, pp. 1–4.
[116] M. R. Akram, G. Ding, K. Chen, Y. Feng, and W. Zhu, "Ultrathin single layer metasurfaces with ultra-wideband operation for both transmission and reflection," *Adv. Mater.*, vol. 32, no. 12, Mar. 2020, Art. no. 1907308.
[117] X. Liu, Z. Yan, E. Wang, X. Zhao, T. Zhang, and F. Fan, "Bifunctional full-space metasurface combining pancharatnam–berry and propagation phases," *IEEE Antennas Wireless Propag. Lett.*, vol. 21, pp. 2110–2114, 2022.
[118] C.-B. Zhang, G.-M. Wang, H.-P. Li, X. Zhang, X.-J. Zou, W.-Y. Ji, and C.-Y. Wang, "Multifunctional full-space metasurface with complete polarization control," *IEEE Access*, vol. 7, pp. 88830–88835, 2019.

[119] J. Zhu and Y. Yang, "3-D printed transmission-reflection-integrated metasurface for spin-decoupled full-space quadruplex channels independent phase modulation," *IEEE Trans. Microw. Theory Techn.*, vol. 72, no. 8, pp. 4790–4800, Aug. 2024.

[120] Y. Wang and A. Zhang, "Dual circularly polarized fabry–perot resonator antenna employing a polarization conversion metasurface," *IEEE Access*, vol. 9, pp. 44881–44887, 2021.

[121] Y. Wang, Y. Ge, Z. Chen, X. Liu, J. Pu, K. Liu, H. Chen, and Y. Hao, "Broadband high-efficiency ultrathin metasurfaces with simultaneous independent control of transmission and reflection amplitudes and phases," *IEEE Trans. Microw. Theory Techn.*, vol. 70, no. 1, pp. 254–263, Jan. 2022.

[122] Y. Jing, "Full-space-manipulated multifunctional coding metasurface based on 'Fabry–Pérot-like' cavity," *Opt Exp.*, vol. 27, no. 27, pp. 21520–21531, 2019.

[123] J. Han, X. Cao, J. Gao, H. Yu, Z. Zhang, and S. Li, "A coding optimized polarization conversion metasurface in broadband and wide-angle," *Int. J. RF Microw. Comput.-Aided Eng.*, vol. 30, no. 5, p. 22061, May 2020.

[124] J. Li, J. Feng, B. Li, H. Shi, A. Zhang, and J. Chen, "Dual-band transmissive cross-polarization converter with extremely high polarization conversion ratio using transmitarray," *Materials*, vol. 12, no. 11, p. 1827, Jun. 2019.

[125] A. K. Fahad, C. Ruan, R. Nazir, M. Saleem, T. U. Haq, S. Ullah, and W. He, "Ultra-thin metasheet for dual-wide-band linear to circular polarization conversion with wide-angle performance," *IEEE Access*, vol. 8, pp. 163244–163254, 2020.

[126] A. K. Fahad, C. Ruan, and K. Chen, "A wideband terahertz transmissive polarization manipulator based on metasurfaces," *Electronics*, vol. 8, no. 10, p. 1068, Sep. 2019.

[127] G. Xu, F. Yu, K. Guo, F. Shen, H. Zhou, Y. Sun, X. Zhang, Z. Yin, and Z. Guo, "Tri-band polarization convertor based on the multi-layer metamaterial," *Appl. Phys. A, Solids Surf.*, vol. 123, no. 10, pp. 1–9, Oct. 2017.

[128] Q. Zhang, J. Wang, R. Xie, Z. Gu, Z. Zhang, X. Wang, H. Zhang, C. Chen, W. Chen, J. Ding, and X. Zhang, "Four-channel joint-polarization-frequency-multiplexing encryption meta-hologram based on dual-band polarization multiplexing meta-atoms," *Opt. Exp.*, vol. 31, no. 11, pp. 17569–17579, 2023.

[129] J.-K. Yang and H.-S. Jeong, "Switchable metasurface with VO2 thin film at visible light by changing temperature," *Photonics*, vol. 8, no. 2, p. 57, Feb. 2021.

[130] Y. Jiang, M. Zhang, W. Wang, and Z. Song, "Reflective and transmissive cross-polarization converter for terahertz wave in a switchable metamaterial," *Phys. Scripta*, vol. 97, no. 1, Jan. 2022, Art. no. 015501.

[131] T. J. Cui, M. Q. Qi, X. Wan, J. Zhao, and Q. Cheng, "Coding metamaterials, digital metamaterials and programmable metamaterials," *Light, Sci. Appl.*, vol. 3, no. 10, p. e218, Oct. 2014.

[132] S. Li, Z. Li, B. Han, G. Huang, X. Liu, H. Yang, and X. Cao, "Multifunctional coding metasurface with left and right circularly polarized and multiple beams," *Frontiers Mater.*, vol. 9, pp. 1–9, Feb. 2022.

[133] Y. Pan, F. Lan, Y. Zhang, H. Zeng, L. Wang, T. Song, G. He, and Z. Yang, "Dual-band multifunctional coding metasurface with a mingled anisotropic aperture for polarized manipulation in full space," *Photon. Res.*, vol. 10, no. 2, p. 416, 2022.

[134] L. Zhu, T. Li, L. Dong, H. Li, W. Zhou, and C. Zhao, "Polarization-controlled multifunctional coding metasurface operating in transmission-reflection modes," *Optik*, vol. 242, Sep. 2021, Art. no. 167288.

[135] L. Zhang, R. Y. Wu, G. D. Bai, H. T. Wu, Q. Ma, X. Q. Chen, and T. J. Cui, "Transmission-reflection-integrated multifunctional coding metasurface for full-space controls of electromagnetic waves," *Adv. Funct. Mater.*, vol. 28, no. 33, pp. 1–9, Aug. 2018.

[136] H. Zhu, M. Yu, Y. Zhou, G. Wang, Y. Di, K. Wang, L. Liu, and S. Xie, "Transmission and reflection bidirectional terahertz coding metasurface based on thermally switchable materials," *Opt. Commun.*, vol. 550, Jan. 2024, Art. no. 129855.

[137] W.-L. Guo, G.-M. Wang, H.-S. Hou, K. Chen, and Y. Feng, "Multifunctional coding metasurface for dual-band independent electromagnetic wave control," *Opt. Exp.*, vol. 27, no. 14, pp. 19196–19211, 2019.

[138] M. Xiang, "Simultaneous transmitting and reflecting reconfigurable array (STAR-RA) with independent beams," *IEEE Trans. Antennas Propag.*, vol. 71, pp. 8338–8343, 2023.

[139] Y. Liu, X. Mu, J. Xu, R. Schober, Y. Hao, H. V. Poor, and L. Hanzo, "STAR: Simultaneous transmission and reflection for 360° coverage by intelligent surfaces," *IEEE Wireless Commun.*, vol. 28, no. 6, pp. 102–109, Dec. 2021.

[140] E. Vassos, J. Churm, and A. Feresidis, "Ultra-low-loss tunable piezoelectric-actuated metasurfaces achieving 360° or 180° dynamic phase shift at millimeter-waves," *Sci. Rep.*, vol. 10, no. 1, p. 15679, Sep. 2020.

[141] S. Zahra, L. Ma, W. Wang, J. Li, D. Chen, Y. Liu, Y. Zhou, N. Li, Y. Huang, and G. Wen, "Electromagnetic metasurfaces and reconfigurable metasurfaces: A review," *Frontiers Phys.*, vol. 8, Jan. 2021, Art. no. 593411.

[142] P. H. Z. Cano, E. Vassos, Z. D. Zaharis, P. I. Lazaridis, T. V. Yioultsis, N. V. Kantartzis, and A. P. Feresidis, "Ultralow-loss reconfigurable phase-shifting metasurface in V band: A multiobjective optimization approach," *IEEE Trans. Antennas Propag.*, vol. 72, pp. 1407–1417, 2024.

[143] Y. Mu, C. Pang, Y. Wang, Q. Wang, and J. Qi, "Complex-amplitude radiation-type metasurface enabling beamform-controlled energy allocation," *Photon. Res.*, vol. 11, no. 6, pp. 986–998, 2023.

[144] Y. H. Liu, S. Y. Wang, K. N. Qi, and Y. B. Li, "Dynamic controlling the bistatic RCS by programmable metasurface with continuous and independent manipulation of reflective phase and amplitude," *IEEE Antennas Wireless Propag. Lett.*, vol. 23, pp. 1000–1004, 2024.

[145] M. Soltani and G. V. Eleftheriades, "Wide-angle impedance matching of a patch antenna phased array using artificial dielectric sheets," *IEEE Trans. Antennas Propag.*, vol. 72, no. 5, pp. 4258–4270, May 2024.

[146] M. Alibakhshikenari, B. S. Virdee, C. H. See, R. A. Abd-Alhameed, F. Falcone, and E. Limiti, "Impedance matching network based on metasurfaces (2-D metamaterials) for electrically small antennas," in *Proc. IEEE Int. Symp. Antennas Propag. North Amer. Radio Sci. Meeting*, Jul. 2020, pp. 1953–1954.

[147] A. Asim, M. Cada, Y. Ma, and A. Fine, "Dual-resonance split ring resonator metasurface for terahertz biosensing," *IEEE Sensors J.*, vol. 24, no. 9, pp. 14189–14196, May 2024.

[148] H. Zeng, S. Gong, L. Wang, T. Zhou, Y. Zhang, F. Lan, X. Cong, L. Wang, T. Song, Y. Zhao, Z. Yang, and D. M. Mittleman, "A review of terahertz phase modulation from free space to guided wave integrated devices," *Nanophotonics*, vol. 11, no. 3, pp. 415–437, Jan. 2022.

[149] C.-Y. Hsu, Z. Pei, and J.-M. Liu, "High-efficiency broadband infrared thin-film germanium photodetector enhanced by a resonant cavity and a nano-slit metasurface," *IEEE Access*, vol. 12, pp. 156904–156914, 2024.

[150] M. A. Shameli, M. Magarotto, A. D. Capobianco, L. Schenato, M. Santagiustina, M. A. Vincenti, and D. de Ceglia, "Reconfigurable and broadband analog computing with terahertz metasurface based on electrical tuning of vanadium-dioxide resonators," *IEEE Access*, vol. 12, pp. 170478–170486, 2024.

[151] T. Huang, Z. Wu, S. Huang, Z. Wen, W. Jiang, J. Xu, J. Wang, and Y. Luo, "Broadband transreflective metasurface for multifunctional dual-band OAM engineering," *IEEE Trans. Antennas Propag.*, vol. 72, no. 9, pp. 7041–7047, Sep. 2024.

[152] B. Li, Y. Chen, S. Yu, X. Zhou, Q. Wu, J. Wang, Y. Li, and F. Li, "Ultra-thin broadband circular polarization conversion metasurface for full-space wavefront manipulation application," *IEEE Photon. J.*, vol. 15, no. 4, pp. 1–9, Aug. 2023.

[153] W. Li, H. Guo, X. Wang, G. M. Yang, and Y. Q. Jin, "A 2-bit reconfigurable metasurface with real-time control for deflection, diffusion, and polarization," *IEEE Trans. Antennas Propag.*, vol. 72, no. 2, pp. 1521–1531, Feb. 2024.

[154] Y. Hu, X. Wang, X. Luo, X. Ou, L. Li, Y. Chen, P. Yang, S. Wang, and H. Duan, "All-dielectric metasurfaces for polarization manipulation: Principles and emerging applications," *Nanophotonics*, vol. 9, no. 12, pp. 3755–3780, Sep. 2020.

[155] Y. Jiao, H. Shi, X. Chen, J. Yi, J. Chen, A. Zhang, Z. Xu, and H. Liu, "Polarization-correlation-based metasurface for full-space independent amplitude and phase modulation," *IEEE Trans. Antennas Propag.*, vol. 72, no. 5, pp. 4670–4675, May 2024.

[156] H. L. Phan, T. Q. H. Nguyen, and J.-M. Kim, "Multi-functional wideband metasurface: Perfect absorber and linear to linear and linear to circular polarization converter," *IEEE Access*, vol. 12, pp. 11664–11673, 2024.

[157] L. Wang, H. Shi, J. Yi, L. Dong, H. Liu, A. Zhang, and Z. Xu, "High-efficiency conversion from rectangular waveguide mode to spoof SPP using metasurface," *IEEE Photon. Technol. Lett.*, vol. 34, no. 15, pp. 783–786, Aug. 2022.

[158] S. Zong and J. Liang, "Broadband high-efficiency co-polarized wavefront manipulation based on multi-layered metasurface for terahertz wave," *IEEE Access*, vol. 12, pp. 45299–45308, 2024.
[159] Z. Ren, Y. Q. Liu, Y. Wang, L. Lu, K. Qi, and H. Yin, "Ultra-broadband RCS reduction based on optimized coding 'whale-shaped' polarization conversion metasurface with angular stability," *IEEE Access*, vol. 10, pp. 50479–50486, 2022.
[160] T.-L. Vu and C. Seo, "A high angular stability, single-layer transmission linear-to-circular polarization converter for dual ISM-band operation," *IEEE Access*, vol. 11, pp. 30188–30196, 2023.
[161] M. Yan, X. Xiu, J. Liu, H. Chen, S. Feng, Q. Xue, and W. Che, "Polarization-insensitive high-angular stable frequency selective surfaces based on anisotropic artificial electromagnetic medium," *IEEE Trans. Microw. Theory Techn.*, vol. 73, no. 2, pp. 1094–1104, Feb. 2025.
[162] Z. Chu, T. Li, J. Wang, Y. Jia, J. Jiang, R. Zhu, L. Li, and S. Qu, "Polarization-multiplexed full-space metasurface simultaneously merging with an ultrawide-angle antireflection and a large-angle retroreflection," *Opt. Exp.*, vol. 30, no. 25, pp. 45776–45791, 2022.
[163] Z. Liu, Z. Wang, T. Li, J. Gu, Y. Shi, J. Zhang, H. Sun, and J. Wang, "Transmission-reflection-integrated bifunctional metasurface by hybridizing geometric phase and propagation phase," *Electronics*, vol. 14, no. 21, p. 4250, Oct. 2025.
[164] J. Zhao, S. Pang, and J. Zhou, "Matching the dual functions of vanadium dioxide metasurfaces through switchable Fabry–Perot structure," *Opt. Mater.*, vol. 146, Dec. 2023, Art. no. 114600.
[165] R. Gao, M.-Q. Yang, Q.-Y. Guo, and W. He, "A low-profile and high-gain antenna with bidirectional beams enabled by integrating folded transmitarray and Fabry–Perot cavity," *IEEE Trans. Antennas Propag.*, vol. 72, no. 8, pp. 6209–6218, Aug. 2024.
[166] X. Liu, S. Li, H. Yang, T. Li, K. Ji, K. Gao, Z. Guo, and Z. Zhang, "Transmission-reflection multifunctional 2-bit coding metasurface with multiple beams," in *IEEE MTT-S Int. Microw. Symp. Dig.*, Nov. 2023, pp. 1–3.
[167] H. Su, X. Xi, Y. Yang, J. Liu, and H. Hu, "Solid-state plasma reconfigurable terahertz metasurface for integrated spatial-amplitude-phase-frequency modulation," *IEEE Trans. Antenna Propag.*, vol. 73, no. 10, pp. 7841–7849, Oct. 2025.
[168] Y. Li, Y. Wang, and Q. Cao, "Design of a multifunctional reconfigurable metasurface for polarization and propagation manipulation," *IEEE Access*, vol. 7, pp. 129183–129191, 2019.
[169] P. Wang, Y. Zhang, Y. Wang, H. C. Zhou, and Z.-M. Yan, "Multifunctional polarization converter based on multilayer reconfigurable metasurface," *Defence Technol.*, vol. 28, pp. 136–145, May 2023.
[170] Z. Shen, Q. Zhang, X. Huang, J. Wu, and H. Yang, "Simultaneous transmissive and reflective polarization conversion cross different operating bands in a single metasurface," *Opt. Laser Technol.*, vol. 169, Feb. 2024, Art. no. 110071.
[171] J. Xu, Y. Liu, X. Mu, and O. A. Dobre, "STAR-RISs: Simultaneous transmitting and reflecting reconfigurable intelligent surfaces," *IEEE Commun. Lett.*, vol. 25, no. 9, pp. 3134–3138, Sep. 2021.
[172] L.-H. Shen, P. C. Wu, C. J. Ku, Y. T. Li, K. T. Feng, Y. Liu, and L. Hanzo, "D-STAR: Dual simultaneously transmitting and reflecting reconfigurable intelligent surfaces for joint uplink/downlink transmission," *IEEE Trans. Commun.*, vol. 72, no. 6, pp. 3305–3322, Jun. 2024.
[173] Z. R. Omam, A. Bagheri, S. Danesh, S. E. Hosseininejad, O. Yurduseven, G. C. Alexandropoulos, and M. Khalily, "STAR-RIS for simultaneous communications and Fourier-based AoA sensing: Design and experimentation," *IEEE Antennas Wireless Propag. Lett.*, vol. 24, no. 11, pp. 4348–4352, Nov. 2025.
[174] H.-F. Huang and S.-N. Li, "High-efficiency planar reflectarray with small-size for OAM generation at microwave range," *IEEE Antennas Wireless Propag. Lett.*, vol. 18, pp. 432–436, 2019.
[175] H.-H. Lv, Q.-L. Huang, X.-J. Yi, J.-Q. Hou, and X.-W. Shi, "Low-profile transmitting metasurface using single dielectric substrate for OAM generation," *IEEE Antennas Wireless Propag. Lett.*, vol. 19, no. 5, pp. 881–885, Sep. 2020.
[176] D. Zhang, X. Cao, J. Gao, H. Yang, W. Li, T. Li, and J. Tian, "A shared aperture 1 bit metasurface for orbital angular momentum multiplexing," *IEEE Antennas Wireless Propag. Lett.*, vol. 18, pp. 566–570, 2019.
[177] G. Li, H. Shi, J. Yi, B. Li, A. Zhang, and Z. Xu, "Transmission–reflection-integrated metasurfaces design for simultaneous manipulation of phase and amplitude," *IEEE Trans. Antennas Propag.*, vol. 70, no. 7, pp. 6072–6077, Jul. 2022.
[178] H. Yi, S.-W. Qu, K.-B. Ng, C. K. Wong, and C. H. Chan, "Terahertz wavefront control on both sides of the cascaded metasurfaces," *IEEE Trans. Antennas Propag.*, vol. 66, no. 1, pp. 209–216, Jan. 2018.
[179] X. Mu, Y. Liu, L. Guo, J. Lin, and R. Schober, "Simultaneously transmitting and reflecting (STAR) RIS aided wireless communications," *IEEE Trans. Wireless Commun.*, vol. 21, no. 5, pp. 3083–3098, May 2022.
[180] W.-L. Guo, K. Chen, G.-M. Wang, X.-Y. Luo, Y.-J. Feng, and C.-W. Qiu, "Transmission–reflection-selective metasurface and its application to RCS reduction of high-gain reflector antenna," *IEEE Trans. Antennas Propag.*, vol. 68, no. 3, pp. 1426–1435, Mar. 2020.
[181] J. L. Wu, Y. M. Pan, and S. Y. Zheng, "Design of single-layer polarization-dependent transmissive and reflective focusing metasurface," *IEEE Trans. Antennas Propag.*, vol. 69, no. 11, pp. 7637–7646, Nov. 2021.
[182] Y. Li, Q. Cao, and Y. Wang, "A wideband multifunctional multilayer switchable linear polarization metasurface," *IEEE Antennas Wireless Propag. Lett.*, vol. 17, pp. 1314–1318, 2018.
[183] M. S. Wahidi, M. I. Khan, F. A. Tahir, and H. Rmili, "Multifunctional single layer metasurface based on hexagonal split ring resonator," *IEEE Access*, vol. 8, pp. 28054–28063, 2020.
[184] J. Yang, X. Wu, J. Song, C. Huang, Y. Huang, and X. Luo, "Cascaded metasurface for simultaneous control of transmission and reflection," *Opt. Exp.*, vol. 27, no. 6, pp. 9061–9070, 2019.
[185] H. Chu, X. Xiong, Y.-J. Gao, J. Luo, H. Jing, C.-Y. Li, R. Peng, M. Wang, and Y. Lai, "Diffuse reflection and reciprocity-protected transmission via a random-flip metasurface," *Sci. Adv.*, vol. 7, no. 37, Sep. 2021, Art. no. eabj0935.

AHMED ALI UMAR received the B.Eng. degree in computer engineering from the University of Maiduguri (UNIMAID), in 2010, and the M.Eng. degree in computer and microelectronics systems from Universiti Tecknologi Malaysia (UTM), in 2018, where he is currently pursuing the Ph.D. degree in communications engineering. His research interests include electromagnetic wave propagation, RF and microwave technologies, and intelligent metasurfaces.

FARID ZUBIR (Member, IEEE) received the B.Eng. degree in electrical, majoring in telecommunication, and the M.Eng. degree in RF and microwave from Universiti Teknologi Malaysia (UTM), in 2008 and 2010, respectively, and the Ph.D. degree from the University of Birmingham, U.K., in 2016. His Ph.D. research focused on the direct integration of power amplifiers with antennas in microwave transmitters. He is currently an Assistant Professor with the Department of Communication Engineering, Faculty of Electrical Engineering, UTM, and a Research Fellow with the Wireless Communication Centre, UTM. He was an Honorary Postdoctoral Research Fellow with The University of British Columbia (UBCO), Okanagan, Canada, from 2019 to 2021, where he conducted research on highly efficient and linear amplification power amplifier topology for wireless power systems. His research interests include RF and microwave technologies, including planar array antennas, dielectric resonator antennas (DRA), active integrated antennas (AIA), RF circuits and devices, beamforming networks, and power amplifiers.

MOHD FAIRUS MOHD YUSOFF received the Bachelor of Engineering degree in electrical telecommunication and the Master's of Electrical Engineering degree in electrical-electronics and telecommunications from Universiti Teknologi Malaysia, in 2002 and 2005, respectively, and the Ph.D. degree in signal processing and telecommunications from the University of Rennes 1, France, in 2012. He joined UTM as a Tutor, in 2002. He is currently a Graduate Faculty Member with the Faculty of Electrical Engineering, UTM. His research interests include antenna design, millimeter waves, and microwave devices.

MUHAMMAD INAM ABBASI (Senior Member, IEEE) received the B.Sc. degree in electrical engineering (telecommunication) from the Centre for Advanced Studies in Engineering (CASE Islamabad), University of Engineering and Technology (UET), Taxilla, Pakistan, in 2008, and the Master's by Research and Ph.D. degrees in electrical engineering from Universiti Tun Hussein Onn Malaysia (UTHM), in 2011 and 2016, respectively. He joined the Wireless and Radio Science Centre (WARAS), UTHM, as a Graduate Research Assistant, in 2009. He was a Postdoctoral Research Fellow with the Wireless Communication Centre (WCC), Universiti Teknologi Malaysia (UTM), from 2017 to 2018. Currently, he is a Senior Lecturer with the Faculty of Electrical and Electronic Engineering Technology, Universiti Teknikal Malaysia Melaka (UTeM). He has published one book and more than 80 research papers in internationally indexed journals and conferences. His research interests include high-performance planar and printed antenna design, passive and reconfigurable reflectarray and planar reflector antennas, and novel materials for the design of enhanced performance antennas.

SHAHARIL MOHD SHAH (Member, IEEE) received the B.Eng. degree in microwave and communication from Multimedia University (MMU), in 2002, the M.Sc. degree in microwave engineering and wireless subsystems design from the University of Surrey, U.K., in 2004, and the Ph.D. degree in communication engineering from the University of Birmingham, U.K., in 2016. He is currently an Associate Professor with the Department of Communication Engineering, Faculty of Electrical and Electronic Engineering, Universiti Tun Hussein Onn Malaysia (UTHM). His research interests include, but not limited to design of microwave devices, active antennas measurement, and the nonlinear characterization of active devices.

ARSHAD KARIMBU VALLAPPIL received the B.Tech. degree in electronics and communication engineering from the University of Calicut, Kerala, India, in 2009, the M.Tech. degree in electronics engineering from Pondicherry University, Puducherry, India, in 2013, and the Ph.D. degree in electrical from Universiti Teknologi Malaysia, in 2021. From 2023 to 2025, he was a Researcher with the Institute of Space Science (CSIC-ICE), Spain, on the MIRROR Project (''Measuring Deep Soil Moisture from Drones''). He is currently an Assistant Professor with the Islamic University of Madinah, Madinah, Saudi Arabia. His research interests include RF and microwave systems, antenna arrays, beamforming networks, metamaterials, and metasurfaces.

MAHER ASSAAD received the master's degree in electrical engineering/microelectronics IC design from the University of Montreal, Montreal, Canada, in 2002, and the Ph.D. degree in electrical engineering/microelectronics IC design from The University of Glasgow, Glasgow, U.K., in 2009. He was a Senior Lecturer in electrical engineering with the University Technology of PETRONAS, Malaysia, and an Associate Professor of electronic and communication engineering with the American University of Ras Al Khaimah, United Arab Emirates. He is currently a Professor of electrical and computer engineering with Ajman University, United Arab Emirates. His research interests include the design of circuits/integrated circuits for various type of sensors and for wireline and optical communication systems.

NOORLINDAWATY MD JIZAT (Member, IEEE) received the B.E. and M.S. degrees in electrical engineering (telecommunication) from Universiti Teknologi Malaysia (UTM), in 2008 and 2010, respectively, and the Ph.D. degree in electrical engineering (telecommunication) from Multimedia University (MMU), Malaysia, in 2024. From 2008 to 2012, she was a Quality Engineer with Flextronics Technology Pvt. Ltd., and a Research and Development Engineer with Panasonic System Network Malaysia. She is currently with MMU, as a Lecturer/Researcher with the Faculty of Artificial Intelligence and Engineering. Her research interests include beamforming networks, butler matrix, beam steering, antenna array, self-powered solar Wi-Fi systems, and material research into antenna applications.